HOLLERS, BRADLEY CHRISTOPHER, M.S. Investigation into the Inhibition of Drug-Metabolizing Cytochrome P450 Isoenzymes by the Amazonian Acai Berry (Euterpe oleracea). (2014)
Directed by Dr. Gregory M. Raner. 72 pp.

Natural products, often containing a magnitude of unidentified constituents, have come under scrutiny in order to understand their effects on the human body. Cytochrome P450 enzymes, due to their non-selective nature, are highly susceptible to interference when multiple organic compounds are present in their metabolic environment. These enzymes are responsible for the oxidation of xenobiotic compounds, and thus play a crucial role in phase I drug metabolism. As part of a collaborative project at UNCG, the Amazonian acai berry (*Euterpe oleracea*) is being investigated for bioactive constituents based on a bioassay-guided fractionation strategy. For this study, these acai berry fractions underwent an inhibition-directed screening process against several in vitro human-model CYP450 assays. No remarkable inhibition was observed by the crude acai berry fractions for the CYP3A4 and 2D6 model assays. The 7-methoxycoumarin O-demethylation assay yielded noteworthy inhibition from chloroform-extracted acai berry constituents. Further fractionation was successfully carried out, leading to the discovery of several sub-fractions with substantial inhibition. The 78-D fraction, in particular, was found to contain the fatty acid 1-9-hexadecenoate and gave a K_i value of 73 µM. Such results give strength to the implication that a number of constituents in the acai berry could interfere with drug metabolism of one or more cytochrome P450 isoenzymes.

INVESTIGATION INTO THE INHIBITON OF DRUG-METABOLIZING CYTOCHROME P450 ISOENZYMES BY THE AMAZONIAN ACAI BERRY (EUTERPE OLERACEA)

by

Bradley Christopher Hollers

A Thesis Submitted to
the Faculty of The Graduate School at
The University of North Carolina at Greensboro
in Partial Fulfillment
of the Requirements for the Degree
Master of Science

Greensboro
2014

Approved by

_____

Committee Chair

APPROVAL PAGE

This thesis written by Bradley Christopher Hollers has been approved by the following committee of the Faculty of The Graduate School at The University of North Carolina at Greensboro.

Committee Chair _____

Committee Members _____

_____

_____
Date of Acceptance by Committee

_____
Date of Final Oral Examination

TABLE OF CONTENTS

Page

LIST OF TABLES

Page

LIST OF FIGURES

Page

LIST OF EQUATIONS

Page

LIST OF SCHEMES

Page

CHAPTER I

INTRODUCTION

1.1.0 Xenobiotic Metabolism

The metabolism of xenobiotic compounds in the human body is of tremendous physiological significance. This process facilitates the biotransformation of lipid-soluble foreign molecules into polar, secretable species. This allows for the detoxification of potentially harmful compounds from the body[1].This pathway is divided into two phases. In phase I, enzymes transform the foreign compounds primarily via oxidation, hydrolysis, or oxygenation. In phase II, the compounds are usually conjugated to other hydrophilic cellular components such as glucose, sulfate, or glutathione, which further facilitates their removal[2].

One of the major classes of phase I enzymes is cytochrome P450 (CYP450). These enzymes metabolize drugs using a monooxygenase reaction shown in Equation 1. The active site of these enzymes contains a bound heme group, which serves to activate O_2 and direct the transfer of an oxygen atom to a broad range of substrates[3]. A single CYP450 enzyme can bind to a large number of substrates, allowing for a wide breadth of pharmaceutical compounds to be metabolized. When a foreign compound is introduced into the body, its lifetime is often determined by the rate of metabolism by one or more CYP450 enzymes[2].

$$RH + O_2 + NADPH \rightarrow ROH + H_2O + NADP^+$$

Equation 1. Monooxygenase Reaction of Cytochrome P450.

1.2.0 General Properties of Cytochrome P450

Cytochrome P450 enzymes are a class of membrane-bound enzymes found in a wide range of tissue types, including hepatic and enteric tissue[4]. Distinctions between individual CYP450 enzymes (isozymes) are determined by their amino acid sequence, which can influence protein mass, active site ligand availability, and substrate selectivity[5]. Isozymes are typically given a three-character designation that reflects their classification based on gene sequence homology. For example, CYP2D6 is in the '2' family and '2D' subfamily, with the '6' identifying the individual isozyme. Classification of the CYP450 isozymes states that isozymes share >40% homology in a family and >55% homology in a subfamily[6].

The most important aspect of CYP450 structure is the active site. Substrate selectivity is primarily dictated by the polarity and volume of the active site[7]. CYP3A4, for example, has an active site volume estimated at 950 A^3, and can metabolize a wide range of substrates, such as paclitaxel (854 Da) and codeine (300 Da)[8]. CYP2A6, with a much smaller active site estimated at 230 A^3, has a much more narrow range of substrates, including coumarin (146 Da) and nicotine (162 Da)[9]. Despite these distinctions, CYP450 isozymes share a highly conserved iron (III) containing porphyrin ring with a proximal cysteine side chain in their active sites. These analogous structures are important for CYP450's role in the oxidation of organic molecules, and all isozymes appear to share a common catalytic cycle[10].

1.2.1 Catalytic Cycle

When a substrate is introduced to CYP450, the enzyme will initiate a monooxygenase reaction in which an oxygen atom that is derived from molecular oxygen is added to the substrate. Enzyme activity requires the presence of an auxiliary enzyme, CYP450 reductase, which mediates the transfer of electrons from NADPH to the heme complex in the active site. As illustrated in Figure 1, the active site heme is in the ferric state when the catalytic cycle begins (***1***). When an organic substrate enters the active site, it displaces a coordinated water molecule, causing a change in the reduction potential of the iron center and facilitating subsequent transfer of an electron to the ferric Fe^{III} complex, which forms the reduced Fe^{II}(***2***). Upon reduction, the heme complex will form a ferrous-dioxide species by attaching O_2 to the iron center (***3***). The CYP450 reductase transfers another electron, which will again reduce the ferrous-dioxygen complex, transforming it into the ferric peroxo complex (***4***). The oxygen molecule will undergo protonation, followed by heterolytic O-O bond cleavage, releasing a water molecule. Left behind is a high valent iron-oxo complex, which enables the enzyme to now oxidize the substrate (***5***). A water molecule will replace the newly oxidized product in the active site, regenerating the enzyme back into the resting state (***1***)[11]. A proximal cysteine ligand is primarily responsible for assisting in the formation of the high valent iron-oxo species. The thiolate ligand is a good electron donor and exhibits a "push effect" on the iron atom, allowing for the cleavage of the O-O bond and releasing the water molecule[12].

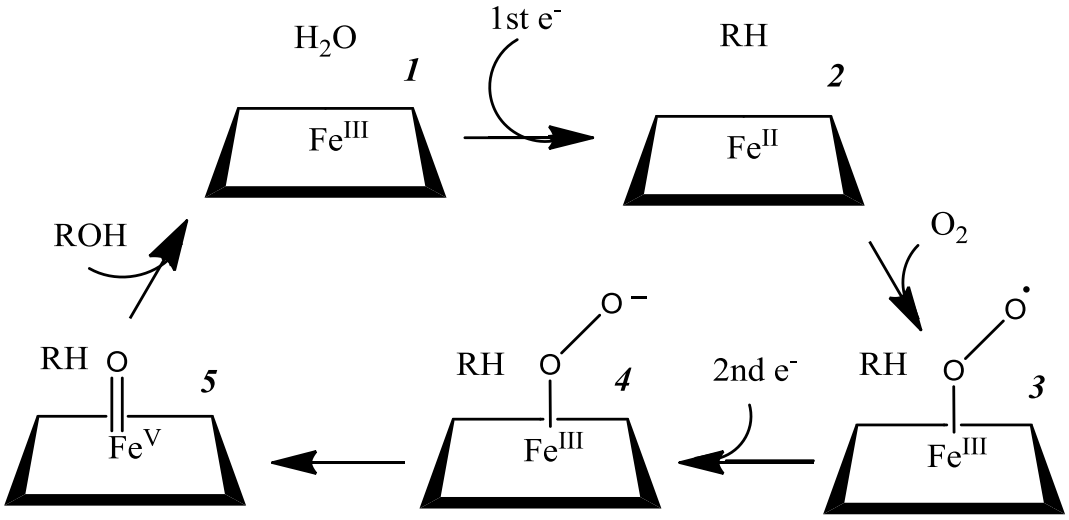

Figure 1. Catalytic Cycle of the CYP450 Monooxygenase Reaction. This catalytic cycle is thought to be operative in nearly all known cytochrome P450 isozymes.

This catalytic cycle lends itself to nearly 30 different types of chemical oxidations that can be carried out by various CYP450 with their respective substrates. These are the result of the radical or concerted reaction between the high valent iron-oxo species and organic substrate, which can then result in a variety of spontaneous modifications after oxygen insertion[11]. Examples of these CYP450 reactions, hydrocarbon hydroxylation and heteroatom dealkylation, are described in the following sections.

1.2.2 Hydrocarbon Hydroxylation

The hydroxylation of a sp3 carbon is perhaps the most basic monooxygenase reaction carried out by CYP450. As shown in Figure 2, the hydroxylation reaction involves a two-step radical pathway, sometimes referred to as the 'oxygen rebound' mechanism. The reaction begins with the alkane substrate oriented above the iron-oxo poryphrin ring, followed by hydrogen atom transfers, leading to the reduction of the oxo-

ferryl group by one electron and leaving behind a radical carbon[13]. 'Oxygen rebound' is then initiated as the transfer of the hydroxyl group on the heme to the carbon radical, forming the final product in tandem with the final reduction of the heme, reverting the enzyme back to its resting ferric state[14].

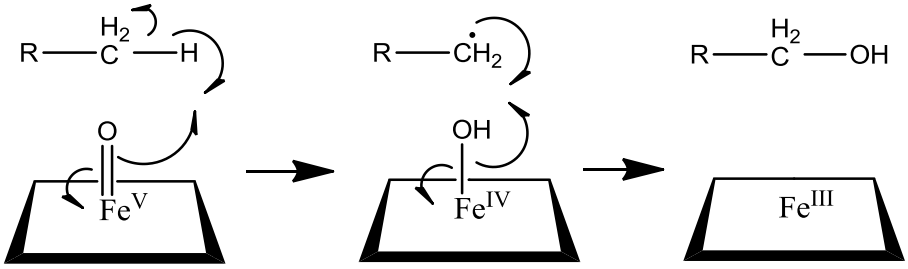

Figure 2. Hydrocarbon Hydroxylation Reaction. This two-step radical reaction is the primary reaction of cytochrome P450.

1.2.3 Heteroatom Dealkylation

This second type of CYP450 reaction illustrates an example of post-enzymatic modification. This reaction is characteristic of substrates whose target carbon is adjacent to an oxygen, nitrogen, or sulfur. As shown in Figure 3, the substrate will undergo normal hydroxylation. The proximity of the hydroxide to the neighboring heteroatom leads to rearrangement and subsequent dealkylation. As a result, a secondary metabolite is formed, typically an aldehyde[15].

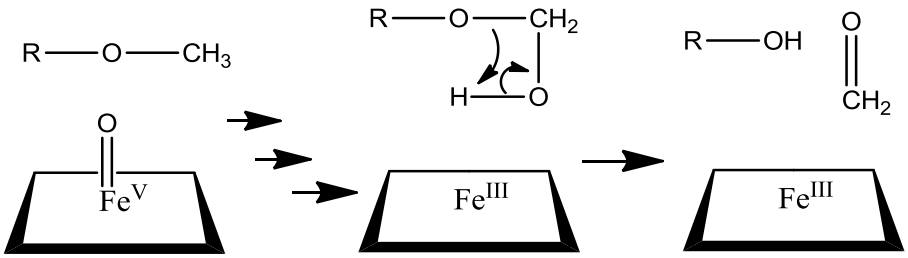

Figure 3. Heteroatom Dealkylation Reaction. This reaction results in the formation of a secondary product, which in this example is formaldehyde.

1.3.0 Kinetics of CYP450 Activity

Many cytochrome P450 enzymes adhere to the Michaelis-Menten model of enzyme kinetics. The key indicator of faithfulness to this model is the Michaelis-Menten plot, which illustrates the relationship between reaction rate V and substrate concentration [S], as seen in Figure 4. In this model, reaction velocity follows a rectangular hyperbolic dependence on the substrate concentration. Eventually, the reaction rate will asymptotically approach a maximum threshold. This terminal velocity, known as the V_{max}, reflects the maximum rate of product formation after complete saturation of available enzyme in the reaction by the substrate. Another constant in the Michaelis Menten plot is the K_m, which is the substrate concentration when the reaction velocity is ½ V_{max}. The K_m reflects a point in the reaction where 50% of the enzyme is bound to substrate, and is an important consideration during optimization of the cytochrome P450 assays, as described in the experiment section.

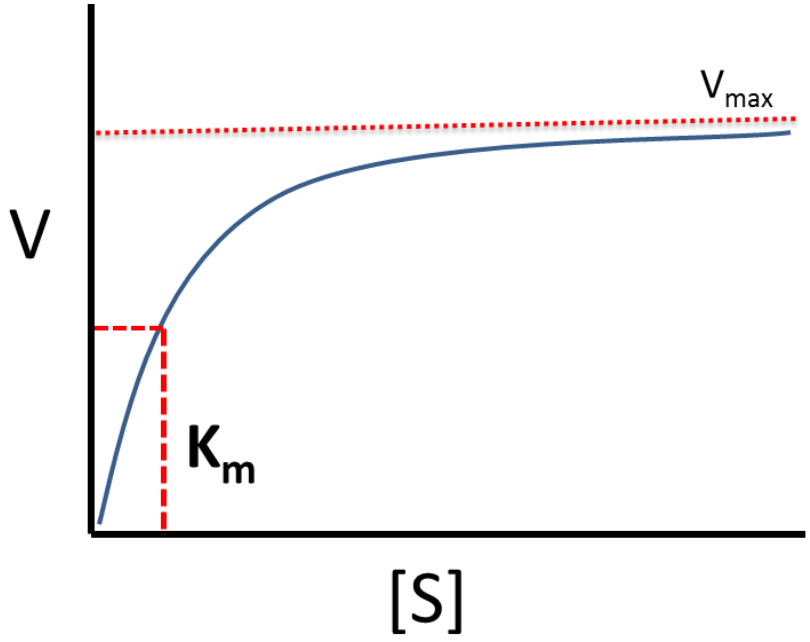

Figure 4. Michaelis-Menten Plot. Illustration showing the nonlinear relationship between reaction rate V and substrate concentration [S], along with the corresponding V_{max} and K_m constants.

1.3.1 Inhibition of CYP450

As previously stated, cytochrome P450 serves the purpose of detoxifying the body of foreign organic molecules, which includes the metabolism of pharmaceutical compounds[1]. Like any enzyme in the body, the activity of CYP450 toward one substrate can be altered by the presence of a competing substrate or related compound.

The focus of this study is on cytochrome P450 inhibition by compounds found in the popular superfruit acai berry. An inhibitor is any molecule that blocks the enzymatic metabolism of another molecule. The term 'drug interaction' can refer to the instance when the metabolism of a drug by CYP450 is inhibited, thus leading to an increase in the drug's bioavailability, thus increasing the possibility of adverse drug effects. Depending

on how it binds to the active site, an inhibitor can be classified into one of two distinct categories: irreversible and reversible.

Irreversible inhibitors, like reversible inhibitors, depend on hydrophobic and/or hydrophilic bonds to bind to the active site. However, these inhibitors may undergo activation by the enzyme and form intermediates that will covalently bind to the heme or amino acid residues in the active site. This form of catalysis-dependent inhibition, also referred to as 'suicide inhibition', will permanently disable the affected enzyme and remove it from the catalytic enzyme pool.

A reversible inhibitor binds to CYP450 prior to substrate oxidation. For the type of inhibitor referred to as 'reversible', the effects last only as long as the inhibitor is present[18]. It binds to the enzyme either through lipophilic attraction to hydrophobic amino acids in the active site cavity or hydrogen bonding. The potency of the inhibitor directly corresponds with the strength of these bonds. Imadazole and pyridine-derivatives with nitrogen-containing aliphatic or aromatic groups typically bind tightly due to their high nucleophilicity, and attraction to the heme iron itself. Alcohols, ketones, and other oxygen-containing compounds have weaker heme-affinities and are considered weak reversible inhibitors.

1.4.0 Drug Interactions in CYP450 Isoenzymes

Studies into cytochrome P450 inhibition is of particular concern in recent years due to the booming pharmaceutical industry flooding the market with thousands of synthetically-produced and naturally-derived drugs. It is no coincidence that, with the increase in prescriptions, there has been an increase in health issues caused by harmful drug interactions[16]. Cytochrome P450 enzymes have a 'non-selective nature', where multiple molecules have a high probability of entering and binding to the active site if they share similar size and polarity as substrates, leading to interactions[17]. The following sections highlight specific cytochrome P450 isoforms most commonly associated with drug interactions.

1.4.1 CYP3A4

Cytochrome P450 3A4 plays a crucial role in human drug metabolism. CYP3A4 enzymes are most abundant in the small intestine and liver, accounting for an estimated 80% of the intestinal CYP450 population, and 40% of the hepatic CYP450 population, making it the most abundant CYP450 isozyme in the human body[17]. The cytochrome P450 3A family is also highly conserved across various mammalian species. Both the rat CYP3A23 and rabbit CYP3A6 enzymes share structural homology with the human CYP3A4 enzyme. These homologs can serve as comparative models in terms of studying their catalytic activity and predicting effects on human CYP3A4[18].

With its abundance, human CYP3A4 supports a very broad selection of pharmaceutical substrates, and is involved in the oxidation of over 60% of the drug market[19]. Table 1 illustrates the vast range of drugs mediated by CYP3A4 metabolism.

Additionally, a list of known potent CYP3A4 inhibitors is shown. It is important to note that substrates of CYP3A4 can simultaneously act as inhibitors through competition with other substrates for the active site[20].

Table 1. List of Common Medications and Inhibitors of CYP3A4

Drugs Metabolized by CYP3A4[21]	Known Inhibitors of CYP3A4[17]
Calcium-channel blockers -felodipine, nifedipine *Chemotherapeutics* -paclitaxel, tamoxifen *Antibiotics* -erythromycin, clarithromycin *Biosynthetic Substrates* -testosterone	*Antifungal azole compounds* -ketocanozole, itraconazole *Antiviral protease inhibitors* -ritonvir, saquinavir *Other antibiotics* -chloramephenicol -clarithromycin, telithromycin

Drug-drug interactions, mediated by the inhibition of CYP3A4, are of particular concern due to the potential of adverse effects. Simvastin (Zocor), a widely prescribed statin-class cholesterol medication, is metabolized solely by CYP3A4. When ingested simultaneously with a known CYP3A4 inhibitor, simvastin will remain in the bloodstream longer than normal, so continued dosing can lead to elevated plasma levels. This increases the risk of statin-induced myopathy, causing degradation of muscle tissue and kidney damage through rhabdomyolysis[22].

1.4.2 CYP2D6

Cytochrome P450 2D6 is another prominent isozyme in the human body. CYP2D6 enzymes mainly occupy the liver, and make up approximately 10 % of the hepatic CYP450 pool[17]. Despite the reduced colonization in the body when compared to CY3A4, CYP2D6 metabolizes about 25% of the known drug market. Most notably, it is responsible for a wide array of drugs that cross the blood-brain barrier[23]. Table 2 lists a selection of known CYP2D6 substrates and inhibitors.

Table 2. List of Common Medications and Inhibitors of CYP2D6.

Drug Metabolized by CYP2D6[24]	Known Inhibitors of CYP2D6[23]
Antidepressants -fluoxetine, paroxeitne (SSRIs) -bufuralol, metoprolol (beta blockers) -imipramine (tricyclic antidepressants) *Other Psychoactive Drugs* -dextromethorphan -codiene, hydrocodone, tramadol	*Other Antidepressants* -bupropion, citralopram -fluxoetine, paroxetine (when combined with other medication) *Other Drugs* -quinidine (antiarrythmic) -ritonavir (protease inhibitor)

An example of an adverse reaction to drug-drug interaction mediated by CYP2D6 is illustrated in the following case study[25]. A patient was admitted to the emergency room for symptomatic hypotension after being prescribed two medications. She was first prescribed paroxetine (Paxil), an SSRI-class antidepressant, to treat her anxiety and panic disorder. Paroxetine also happens to be a strong inhibitor of CYP2D6[26]. Later, after developing an unrelated case of hypertension, she was prescribed a high dose of metoprolol (Toprol XL), an agent that blocks the beta receptors on cardiovascular cells to

reduce stimulation. Metroprolol depends exclusively on CYP2D6 for deactivation and excretion. When inhibited by the SSRI, metroprolol concentration will peak in the cardiovascular tissue. Blood pressure will eventually drop to harmful levels, causing dizziness and loss of consciousness from hypotension[27].

1.4.3 CYP2B6

Cytochrome P450 2B6 is a small, membrane bound enzyme found in the endoplasmic reticulum of liver cells, and composes less than 1% of the hepatic CYP450 population[17]. Due to its comparatively meager stock, CYP2B6 was often considered to have an insignificant role in drug metabolism. However, recent studies have suggested that the enzyme is responsible for the activation of nevirapine and efavirenz, both non-nucleoside reverse transcritptase inhibitors (NNRTIs) used in antiretroviral therapy for the treatment of HIV-1[28]. A listing of additional substrates and inhibitors of CYP2B6 can be found on Table 3.

Table 3. List of Common Medications and Inhibitors of CYP2B6.

Drugs Metabolized by CYP2B6[28]	Known Inhibitors of CYP2B6[23]
NNRTIs -efavirenz, nevirapone *Chemotherapy Agents* -cyclophosamide -N,N',N"- triethylenephosphoramide *Other Drugs* -lidocaine, diazepam	-triethylenethiophosphoramide (chemotherapeutic) -metryrapone (hypercortisolism treatment) -ticlopidine (antiplatelet) -orphendrine (antihistamine)

1.4.4 Non-Selective Cytochrome P450 Probes

Due to the broad substrate selectivity of multiple cytochrome P450 isoforms, it is often useful to probe for potential interactions using non-selective CYP450 substrates. Classic examples of this include ethoxycoumarin and ethoxyresorufin, which can be metabolized by multiple cytochrome P450 isoforms. The use of these substrates for inhibition studies is very well-represented in the literature, and can lead to identification of potential drug interactions. Woodhouse et al used 7-ethoxycoumarin as a probe for monooxygenase activity in liver tissue with primary biliary cirrhosis, observing a decrease in xenobiotic metabolism in microsomes derived from liver in late stage cirrhosis[29]. In another study, Pelkonen et al monitored the effect of cigarette smoking on the induction of cytochrome P450 by measuring 7-ethoxyresorufin O-deethylation activity[30]. In the current study, the substrate 7-methoxycoumarin was selected as a general probe for cytochrome P450 activity, and the relative contributions to its metabolism by different human isoforms were assessed.

1.5.0 Herbal-Drug Interactions

As described previously, the non-selective nature of the cytochrome P450 enzymes creates an environment in which multiple compounds can compete effectively for the active site of the enzyme. Natural products represent a rich source of diverse xenobiotic compounds with the potential to impede drug metabolism[31]. Due to the lack of rigid standards in the production of herbal and botanical supplements, it is common for a single herbal product to contain hundreds of unidentified organic compounds, whose effects on biochemical processes may not be fully investigated[16].

Recently, there has been a focus on investigating the effects of organic extracts from consumer-based herbal and botanical products on specific P450 isozymes. Furanocoumarins, such as bergamottin (BG) and 6',7'-dihydroxybergamottin (DHB), are a particular class of botanical compounds proven to be strong inhibitors of intestinal CYP3A4, *in vivo* (Figure 5)[32]. Grapefruit juice, which contains a high concentration of these compounds, has been classified as a major constituent in CYP3A4 herbal-drug interactions, characteristic in cases when grapefruit juice is consumed simultaneously with medication during breakfast. As a result, the FDA requires cautionary labeling of several CYP3A4-mediating drugs (e.g. simvastatin, lovastatin, felodipine) to prevent adverse drug interactions when combined with grapefruit juice consumption[33]. An in vitro study suggests that BG and DHB are both potent irreversible inhibitors that act independently of substrate concentration[34].

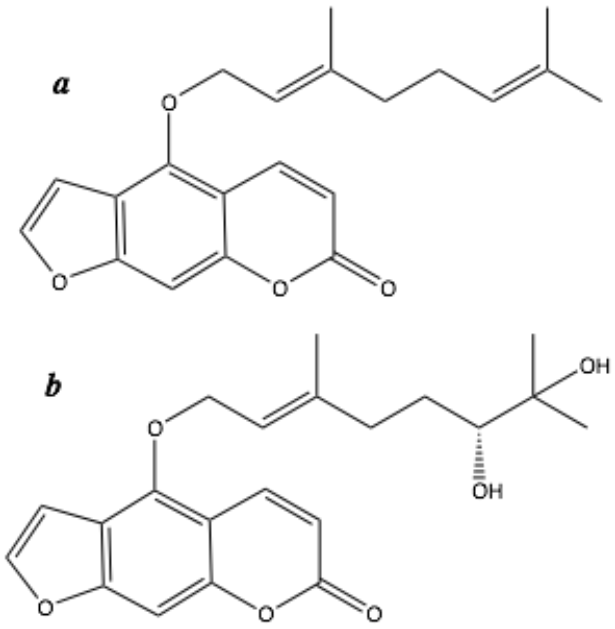

Figure 5. Structures of Bergamottin and 6',7'-Dihydroxybergamottin. Both BG (a) and DHB (b) are natural constituents in grapefruit juice that lead to CYP3A4 inhibition.

1.5.1 Amazonian Acai Berry

With these recent discoveries, this study will focus on the investigation of the inhibitory potential of the Amazonian acai berry (*Euterpe oleracea*) on select cytochrome P450 isozymes involved in drug metabolism. The berry is available in a variety of beverages and has become a popular dietary supplement, with claims of reducing LDL cholesterol levels and supplementing weight-loss[35]. Despite these claims, the acai berry is not listed on the U.S. Food and Drug Administration Generally Recognized As Safe (GRAS) list, as studies into the bioactivity of acai berry constituents is very limited.

Screening of the acai berry pulp and juice by the Cech group at UNCG has shown a strong presence of anthocyanin-class flavonoids, such as cyanidin-3-O-glucoside (C3G) and cyanidin-3-O-rutinoside (C3R). Pharmacokinetic analysis into the oral bioavailability

of acai juice show that plasma anthocyanin concentrations reach a maximum of 1.1-2.3 ng/mL after consuming 18 fl. oz. in an average adult. These compounds have been implicated in the scavenging of free radicals, making acai berry a powerful antioxidant[36]. Additionally, these cyandins have been proven to be modest inhibitors of CYP3A4, with high IC_{50} values (80.2 µM for C3G and 96.1 µM for C3R)[37]. Despite these results, detailed studies aimed at the potential interaction of acai products with human drug-metabolizing CYP450s have not been carried out.

1.6.0 Bioassay-Guided Fractionation

The primary strategy for this study involves the process of bioassay guided fractionation (BGF). The technique incorporates a bioactivity-directed approach in order to separate, isolate, and discover molecules that may have pharmacological or toxicological significance in the body. This method is particular useful in the evaluation of the pharmacognostic properties of natural products, which can contain an enormity of constituents[38].

BGF begins with an initial partitioning of a natural product into crude extracts. Each extract is assayed for interactions in a specific biochemical reaction. Extracts that demonstrate bioactivity are fractionated further, reducing the complexity of constituents in each newly generated fraction. The process repeats until individual bioactive molecules are isolated[39]. One potential drawback to this method involves the inability to identify bioactivity that occurs due to the cooperation of more than one compound. Fractionation could potentially separate these constituents into different extracts, rendering their synergistic bioactivity inoperative and unobservable[40].

Bioassay guided fractionation has proven to be an essential tool in discovering many valuable compounds derived from botanical sources. In 1955, the National Cancer Institute (NCI) commissioned a program to screen more than 114,000 natural products[41]. In a landmark study at the Research Triangle Institute, extracts from endophytic fungi of the Pacific yew tree (*Taxus brevifolia*) were fractionated based on observed anti-leukemic activity. This led to the discovery of paclitaxel, a widely distributed chemotherapeutic agent[42]. In another study utilizing BGF, researchers uncovered an array of beneficial compounds isolated from the unripe South American avocado (*Persea americana*). Fractionation revealed several long chain triols that demonstrated significant cytotoxic selectivity of the PC-3 human prostate carcinoma cell line. The same study also found that one of these compounds exhibited potent lethality towards the larvae of the yellow fever mosquito (*Aedes aegypti*), implying that it could serve as a natural insecticide[43].

This study utilizes BGF in a collaborative effort between several research groups at UNCG that focuses on characterization and identification of bioactive constituents in the acai berry. Freeze-dried acai berry powder from Optimally Organic, Inc. was fractionated into aliquots that were tested for inhibition in cytochrome P450 assays. Fractions that exhibited high inhibitory activity can then be further partitioned by polarity to reduce their complexity. This process continues until the fractions contain single compounds. This strategy utilizes the complimentary expertise of the Raner and Oberlies research groups at UNCG. Robin Tate-Uhl and Tyler Graf, from Dr. Oberlies' laboratory, carried out the fractionation and partitioning of acai berry extracts.

1.7.0 Objective Statement

The goal of this study is to investigate the potential inhibition of several cytochrome P450-mediated reactions by the Amazonian acai berry (*Euterpe olecera*). To this date, there have been no published data showing acai berry inhibition of CYP450. This study is being carried out parallel with another at UNCG in which other isoforms of toxicological significance are the main focus, where preliminary studies have demonstrated inhibitory activity by acai berry extracts toward both CYP 2E1 and 2A6.

CHAPTER II

EXPERIMENTAL

2.1.0 Preparation of Reagents and Stock Solutions

2.1.1 Potassium Phosphate Buffer

A 1 M stock of potassium phosphate buffer was prepared by combining monobasic potassium phosphate and dibasic potassium phosphate, both provided by Carolina Biological Supply Company. The pH of the buffer was adjusted to 7.4 after combining the phosphate solutions. This buffer was used in all CYP450 assays described below as a 10x stock.

2.1.2 NADPH

Nicotinamide adenine dinucleotide phosphate (NADPH), Research Products International (RPI), was dissolved in deionized water and partitioned into 10 mM stock solution aliquots. These aliquots were stored at -80^{o}C until used in CYP450 assays.

2.1.3 Rat Liver Microsomes

Microsomal extractions from rat livers served as a model for hepatic cytochrome P450 enzymes found in humans 15.02 g of frozen rat livers, Pel-Freez Biological in Rogers, AK, were thawed and washed in 60 mL of a buffer consisting of 100 mM potassium phosphate buffer (7.4), 20 % glycerol, 3.3 mM $MgCl_2$, and 0.1 mM EDTA. The tissue and buffer solution were homogenized in a commercial blender in 20 second

bursts. The slurry was centrifuged at 5,000 rpm for 10 minutes. The supernatant was decanted and centrifuged at 25,000 x g for 1 hour. The supernatant was discarded, and the pellet was resuspended and homogenized in 20 mL of the buffer, and stored at -80^{o}C. A Bradford assay was carried out with bovine serum albumin as the standard for generating a calibration curve in order to find the protein concentration of the rat liver microsome stock. The approximate protein concentration was determined to be 15.3 mg/mL.

2.1.4 Human Liver S9 Fractions

Microsomes obtained from the S9 fraction of human liver homogenate were purchased by Molecular Toxicology, Inc., Asheville, NC, and were stored in 60 µL aliquots at -80^{o}C. These microsomes were at a reported concentration of 23.3 mg/mL total protein.

2.1.5 Substrate Stock Solutions

Erythromycin and dextromethorphan were purchased from Sigma, while 7-methoxycoumarin was purchased from Acros Organics. Erythromycin (200 µM), dextromethorphan (200 µM), and 7-methoxycoumarin (1 mM) were dissolved in 10 % methanol, due to their low solubility in H_2O, and stored at room temperature.

2.1.6 Nash Reagent

Nash Reagent was used to quantify the amount of formaldehyde produced in the CYP3A4 and 2D6 reactions. It was prepared using 15 g of ammonium acetate, 200 µL of penta-2,4-dione, and 400 µL glacial acetic acid in a total volume of 50 mL. The solution was stored in a 4^{o}C refrigerator and kept in low light conditions.

2.1.7 Acai Berry Fractions

The acai berry fractions were prepared by collaborators in the Dr. Oberlies research group. Upon arrival, the fractions were divided into aliquots 25-20µg and stored in the refrigerator at 4^{o}C. For study into bioassay inhibition, the fractions were diluted to produce stock solutions between 250-2000 µg/mL. Aqueous and butanol extracted fractions were dissolved in H_2O, while chloroform and hexane extracted fractions were dissolved in 10 % methanol.

2.2.0 Cytochrome P450 Assays

An in vitro reaction assay to test the activity of each CYP450 isoform was first developed before testing the acai berry extracts for inhibition. The approach to develop these assays followed similar protocol to past CYP450 inhibition studies, which include the incubation of purified hepatic microsomes, substrate, NADPH, and buffer (7.4) at 37^{o}C to initiate the monooxygenase reaction. Measuring product formation with variable substrate, microsome, and reaction time suggested that the reactions were linear for up to an hour and obeyed a simple Michaelis-Menten kinetic model.

2.2.1 Nash Reagent Assay

The Nash assay, a reliable method for monitoring reactions that produce formaldehyde as a product, has been used in a number of recent CYP450 studies[44,45,46]. For this study, the Nash assay was utilized to measure activity of the CYP3A4 and 2D6-model assays. This method involves the reaction of 2,4-pentanedione and ammonium acetate with formaldehyde to form 3,5-diacetyl-2,6-dihydolutidine (Figure 6), a yellow

product that can be measured using UV-Vis spectrophotometry at an absorbance wavelength of 412 nm[47].

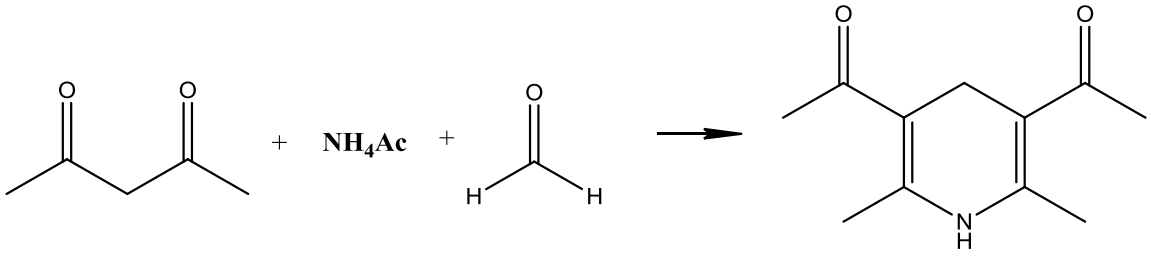

Figure 6. Reaction of the Nash Reagent Assay. Active components in the Nash reagent, 2,4-pentanedione and ammonium acetate, react with formaldehyde to produce a pale yellow chromaphore.

2.2.2 CYP3A4 Model Assay

Rat liver microsomes were used as a source of cytochrome P450 enzymes in this assay. The rat CYP3A2 isoform has been implicated as a model homologue for the human-expressed CYP3A4 enzyme[48,49,50]. Additionally, the CYP3A2 isoform has been shown to metabolize several prominent CYP3A4 substrates, including testosterone[51], erythromycin[49], and midazolam[52]. For this study, the rat CYP3A2 isoform was determined to serves as an adequate model for the human CYP3A4 homologue.

Erythromycin, an antibiotic macrolide, is a commonly used substrate to probe cytochrome P450 3A2 activity. Given its highly selective nature, this compound was elected as the substrate for monitoring CYP3A2 activity. Erythromycin undergoes an N-demethylation to produce a demethylated erythromycin-derivative and formaldehyde, as seen in Figure 7[49].

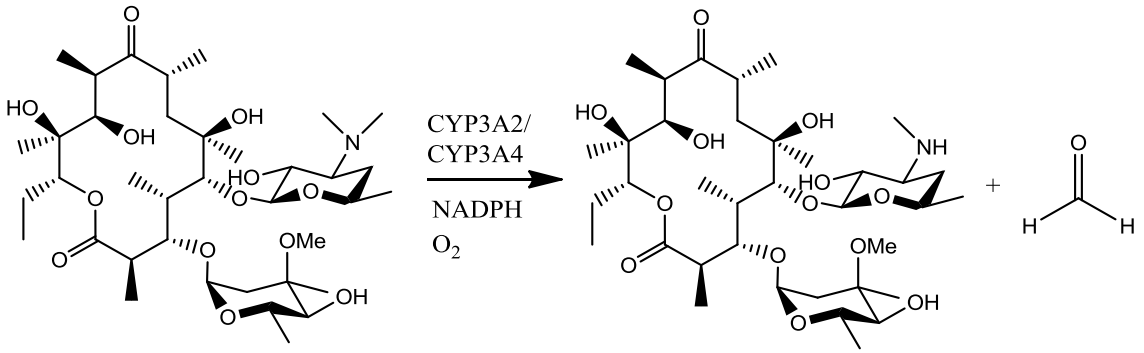

Figure 7. Reaction for Erythromycin N-Demethylation with CYP3A2/3A4. In this reaction, the enzyme utilizes NADPH and O_2 to demethylate the amine group. The formaldehyde product can be quantitated using colorimetric detection.

The erythromycin N-demethylation assay was carried out in 1.5 mL centrifuge tubes using rat liver microsomes (1.1 mg/mL), 10 μM erythromycin, 0.1 M potassium phosphate buffer (7.4), 5 mM $MgCl_2$, and 1 mM NADPH. The reactions were carried out in a final volume of 200 μL. Reactions were initiated with the addition of NADPH, and were incubated at 37°C for 15 minutes. Reactions were terminated with 100 μL of 10% trichloroacetic acid. Samples were chilled in an ice bath for 10 minutes, and then centrifuged at 15,800 g for 10 minutes. Supernatant for each sample was extracted and placed into new centrifuge tubes with 300 μL of Nash reagent. Samples were then incubated at 50°C in low light condition for 30 minutes. Samples were immediately placed into a UV-Vis spectrophotometer (Varian 50 Bio UV-Visible Spectrophotometer) and absorbance was measured at 412 nm. For each analysis, the UV-Vis detector was zeroed via normalization with a 'blank' consisting of all reaction components with the enzyme quenched prior to addition of NADPH to prevent enzyme activity.

2.2.3 CYP2D6 Model Assay

Given the use of rat liver micromsomes in this assay, it's important to mention that the rat CYP2D1 isoform is a confirmed homologue of the human CYP2D6[53,54]. Dextromethorphan, an antitussive found in cough syrup, has been shown to be metabolized by both the CYP2D1[55] and 2D6[56] isoforms. CYP2D1, serving as a model for CYP2D6 in this study, initiates an O-demethylation reaction with the substrate, producing dextrorphan and formaldehyde (Figure 8).

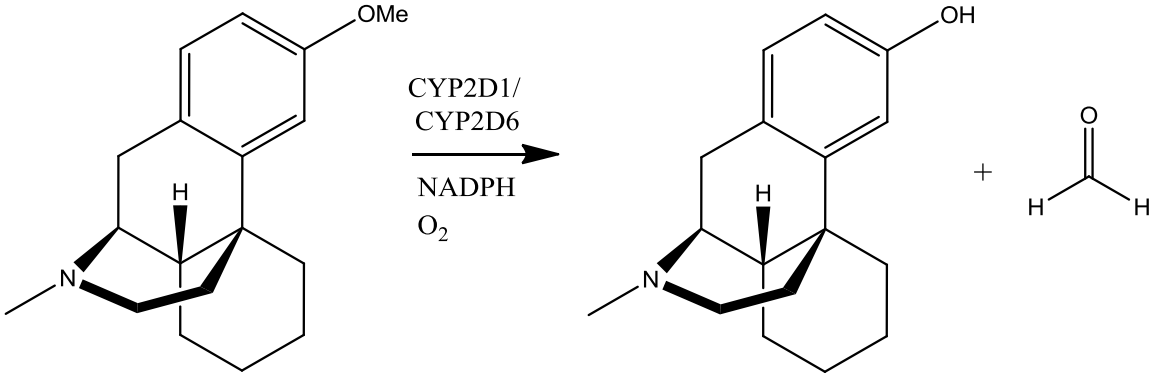

Figure 8. Reaction of Dextromethorphan O-Demethylation with CYP2D1/2D6. This enzyme uses NADPH and O_2 for the demethylation of the ester substituent on dextromethorphan. The formaldehyde product formation can be quantitated using colorimetric analysis.

The dextromethorphan O-demethylation assay was set up in 1.5 mL centrifuge tubes using rat liver microsomes (1.1 µg/mL), 10 µM dextromethorphan, 0.1 M potassium phosphate buffer (7.4), 5 mM $MgCl_2$, and 1 mM NADPH. The samples were diluted in H_2O to a final volume of 200 µL. Reactions were initiated by the addition of NADPH, and were incubated at 37°C for 30 minutes. Reactions were terminated with 100 µL of 10% trichloroacetic acid. Samples were chilled in an ice bath for 10 minutes, and

then centrifuged for 10 minutes at 15,800 g. The supernatant for each sample was extracted and placed into new centrifuge tubes with 300 μL of Nash reagent. Samples were then incubated at 50°C in low light condition for 30 minutes. Samples were immediately placed into a UV-Vis spectrophotometer and absorbance was measured at 412 nm. For each analysis, the UV-Vis detector was zeroed via normalization with a 'blank' consisting of all reaction components with the enzyme quenched prior to incubation to prevent enzyme activity.

2.2.4 7-Methoxycoumarin O-Demethylation (MCOD) Assay

For this assay, human liver CYP450 derived from hepatic S9 fractions were utilized to probe additional cytochrome P450 isozymes. 7-methoxycoumarin was selected as an analytical substrate for probing human CYP450 metabolism due to its fluorogenic properties[57]. The compound is a 7-alkyl derivative of coumarin, a flavenoid used as a synthetic precursor for several anticoagulants[58]. The methoxy group is hydroxylated by cytochrome P450, leading to demethylation and subsequent formation of 7-hydroxycoumarin[57], as seen in Figure 9.

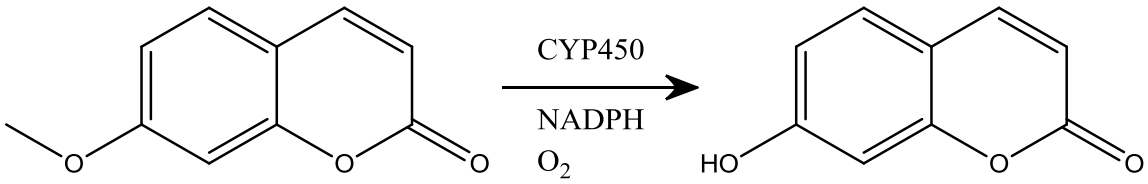

Figure 9. Reaction for 7-Methoxycoumarin O-Demethylation Reaction with Human Liver Microsomes. The product, 7-hydroxycoumarin, is a fluorescent biomarker.

At the beginning of this study, it was assumed that 7-methoxycoumarin O-demethytlation was mediated, in part, by the CYP2B6 due to implications from various studies. Rat CYP2B-class homologues were found to be major metabolizers of 7-methoxycoumarin[59], while human CYP2B6 found to mediate the hydroxylation of several 7-alkycoumarin derivatives[60]. The current study supports this assumption, and has identified additional human isozymes contributing to 7-methoxycoumarin O-demethylation. The literature indicates that phenobarbital-induced cytochrome P450s, which can include a wide range of isozymes from the 2A, 2B, and 2C families[61], have been shown to be predominate metabolizers of the compound, demonstrating an 8-fold increase in product formation versus non-induced microsomes[59]. Additionally, studies have utilized 7-methoxycoumarin as a selective probe for CYP1A2[62] and CYP2A6[63] activity. Our own data and studies indicate 7-methoxycoumarin is a good general probe for CYP450 activity.

The MCOD assay was set up in 1.5 mL centrifuge tubes using S9 fraction of human liver microsomes (0.35 mg/mL), 50 μM 7-methoxycoumarin, 0.1 M potassium phosphate buffer (7.4), and 1 mM NADPH. The samples were diluted in H2O to a final volume of 200 μL. Reactions were initiated with the addition of NADPH, and were incubated at 37^{o}C for 45 minutes. Reactions were terminated with 50 μL of 3% formic acid, then chilled in an ice bath for 10 minutes.

Back extraction was necessary to isolate the organic product prior to fluorescence detection due to the potential interference from NADPH. Following quenching, 400 μL of chloroform were added to each sample. Each tube was vortexed for 30 seconds, then

centrifuged at 14,000 rpm for 5 minutes. 350 µL of the bottom layer organic phase was extracted from each sample and placed in 1000 µL of 30 mM sodium borate (pH 9.2). The samples were vortexed and centrifuged under the same conditions. 1000 µL of the top layer was extracted into a cuvette for fluorescence analysis. The detector in the Varian Cary Eclipse Fluorescence Spectrophotometer was set to excitation wavelength of 360 nm and emission wavelength of 450 nm. For each analysis, the fluorescence baseline was normalized with a 'blank' consisting of all reaction components with the enzyme quenched prior to incubation to prevent enzyme activity.

In the later stages of the study, HPLC was utilized to measure the formation of 7-hydroxcoumarin without using the back extraction method. 50 µL of each sample was injected into a Waters XBridge C_{18} column (4.6 x 150 mm) using a model LC-20AT system (Shimadzu Corp.). An isocratic mobile phase of 20% acetonitrile (with .1% trifluoroacetic acid) and 80% nanopure water (with .1% TFA) was pumped through the system at a rate of 0.600 mL/min. 7-hydroxycoumarin was measured for UV absorbance at 320 nm at a retention time of approximately 6.4 minutes[64].

2.3.0 Initial Partition of Acai Berry Powder

In the initial fractionation of the acai berry powder, solvent partitioning was used to create four crude acai berry fractions. The partitioning process, summarized in Scheme 1, involved dissolving the acai berry powder into a 10:1:9 hexane:H_2O:methanol mixture. The organic phase was extracted from the mixture using a seperatory funnel, isolating highly lipophilic constituents, such as fatty acids and oils. This hexane solution was

aliquoted and dried, producing samples labeled Hexane. The remaining aqueous methanol was mixed with chloroform, producing a 4:1:5 $CHCl_3$:MeOH:H_2O mixture. The organic phase was separated and divided into dried aliquots, producing samples labeled Chloroform. The remaining mixture was mixed with butanol to create a 1:1 BuOH:H_2O mixture. Both the butanol and aqueous layers were separated, aliquoted, and dried to produce the last two samples, labeled Butanol and Aqueous.

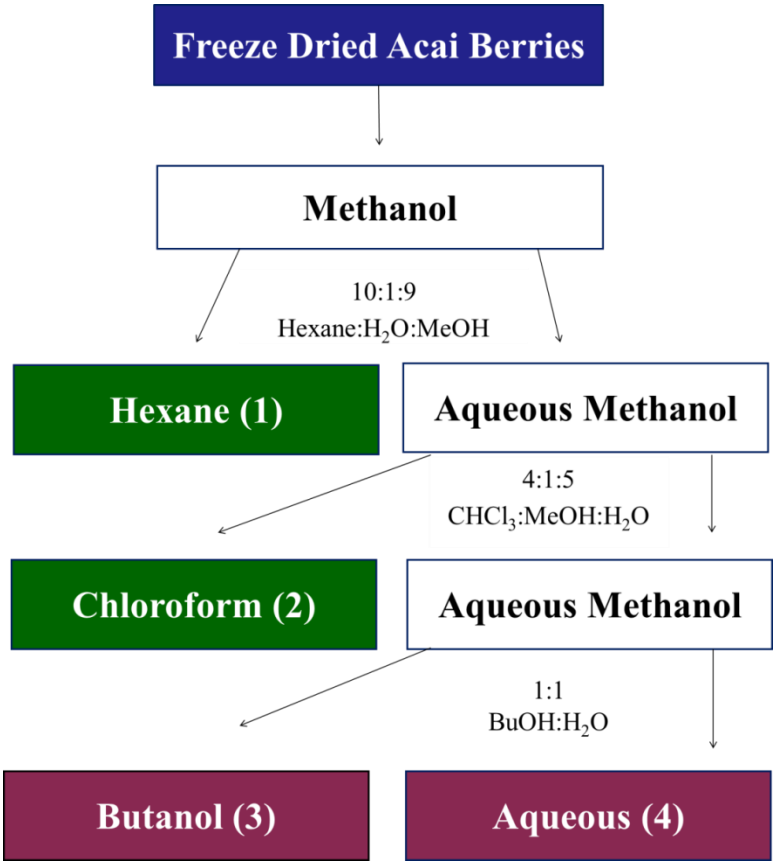

Scheme 1. Generation of Crude Acai Berry Fractions.

2.3.1 Generation of Acai Berry Fractions

Scheme 2 is a diagram of the entire fractionation process throughout the course of this study. Starting with the freeze dried acai berry powder, four crude fractions were generated, as described in the above section. The subsequent fractions were generated using various chromatographic methods by our collaborators in the Oberlies lab (University of North Carolina at Greensboro). The Chloroform sample was fractionated with silica-column flash chromatography (RF CombiFlash) with C_6H_{14}:$CHCl_3$:MeOH solvent gradient, generating the 34 series. The 34-08 sample was fractionated with the same instrument, instead using C_6H_{14}:acetone solvent gradient and producing the 38 series of fractions. The 38-02 sample was subsequently fractionated into the 62 series, using a diol column with C_6H_{14}:ethyl acetate:MeOH gradient. The 62-02 and 62-03 samples were selected to be fractionated into the 78 and 82 series, respectively, as shown in the diagram below. For both fractionations, reverse phase HPLC was used with ACN:H_2O solvent gradient.

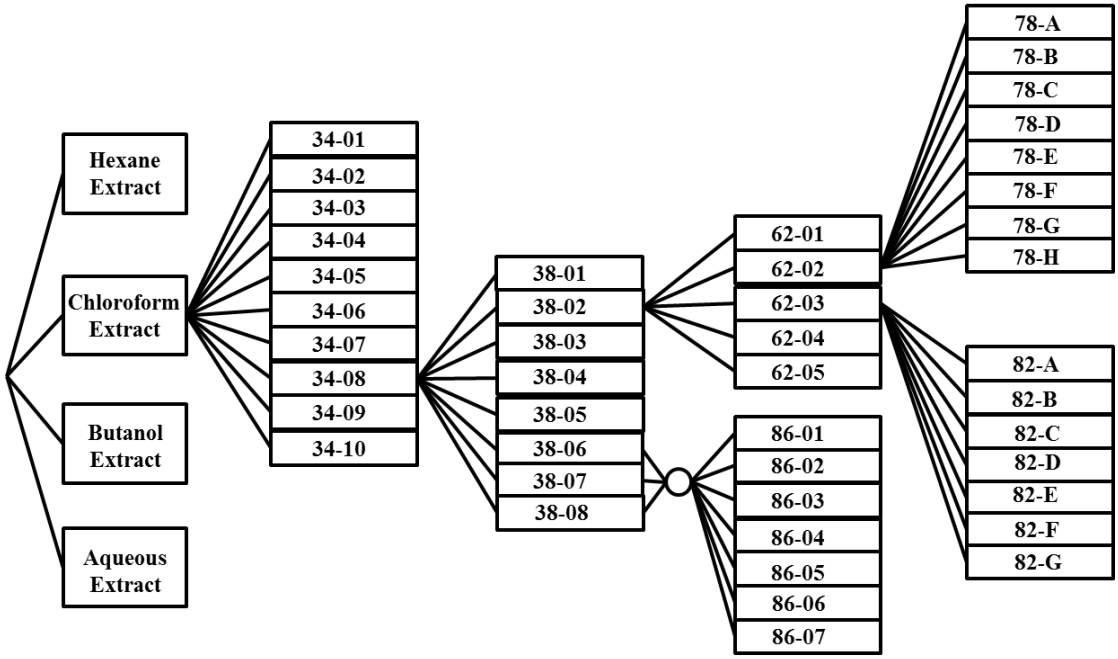

Scheme 2. Summary of Inhibition-Directed Fractionation of Acai Berry Powder. This pathway is based on observed inhibition of the MOCD activity in human liver microsomes.

CHAPTER III

RESULTS AND DISCUSSION

3.1.0 Bioassay Development

While developing the bioassays to measure the activities of each CYP450 isoform, several components of each reaction were tested at variable amounts in order to optimize conditions for the assay. This process included examining the effects of varying enzyme concentration, incubation time, and substrate concentration. Product formation should be linear with time and increase with enzyme concentration in a linear fashion. With varying substrate concentration, the reaction rate should follow a non-linear function in association with Michaelis-Menten kinetics. These steps were taken to ensure that each CYP450 reaction demonstrated enzymatic behavior, as well as optimizing various parameters for each assay before beginning the acai berry inhibition screening.

3.1.1 CYP3A4 Model Assay

The erythromycin N-demethylation reaction was first tested with variable enzyme concentrations. The goal of this experiment was to establish linearity between reaction rate and enzyme concentration, as well as selecting an appropriate volume of rat liver microsomes to use in the subsequent CYP3A4 assays. These reactions were carried out in similar conditions described in the previous chapter. Figure 10 illustrates the results of these reactions, which were tested with 15-45 µL of rat liver microsomes. A linear

increase in activity was observed in correlation with the increase in microsome concentration. Here, the activity was represented in using arbitrary activity units per 30 minute reaction. For optimization, it was decided that 15 µL of rat liver microsomes were to be used in subsequent CYP3A4 reactions. The volume was selected due to the sufficient measurement of activity at a minimal volume, in order to conserve the microsomal stock solution.

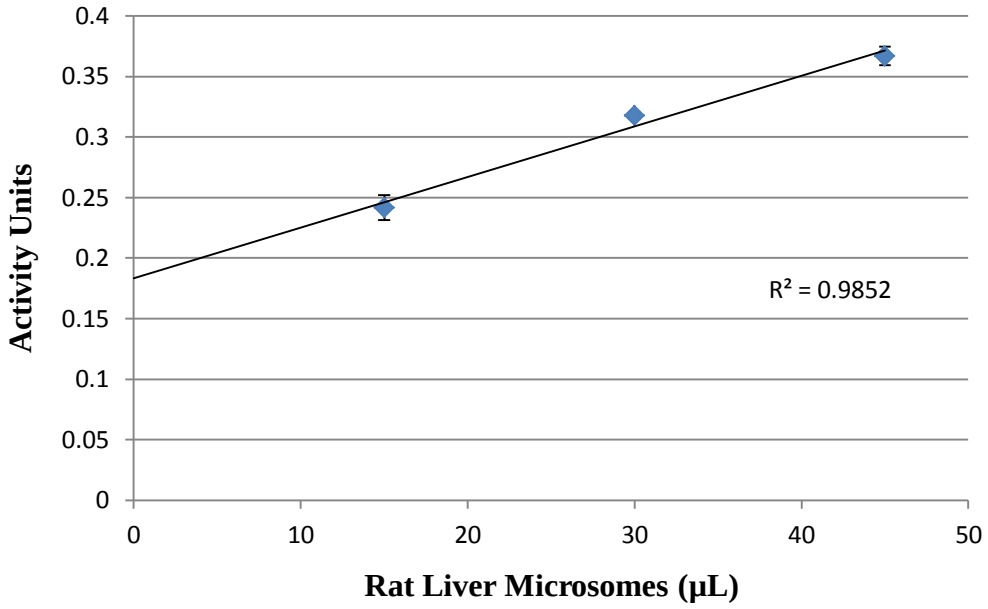

Figure 10. Results for Variation of Microsomal Volume in the CYP3A4 Model Assay.

Additionally, the CYP3A4 reaction was tested with varying reaction times. This involved running reactions under similar conditions with incubation times that varied from 5-20 minutes, the results of which can be seen in Figure 11. Once again, a linear increase in product formation in relation to the increase in reaction time was observed, also indicating that reaction times of 20 or more minutes would be appropriate. For the

acai berry screening, an incubation time of 30 minutes was decided upon for the CYP3A4 assay.

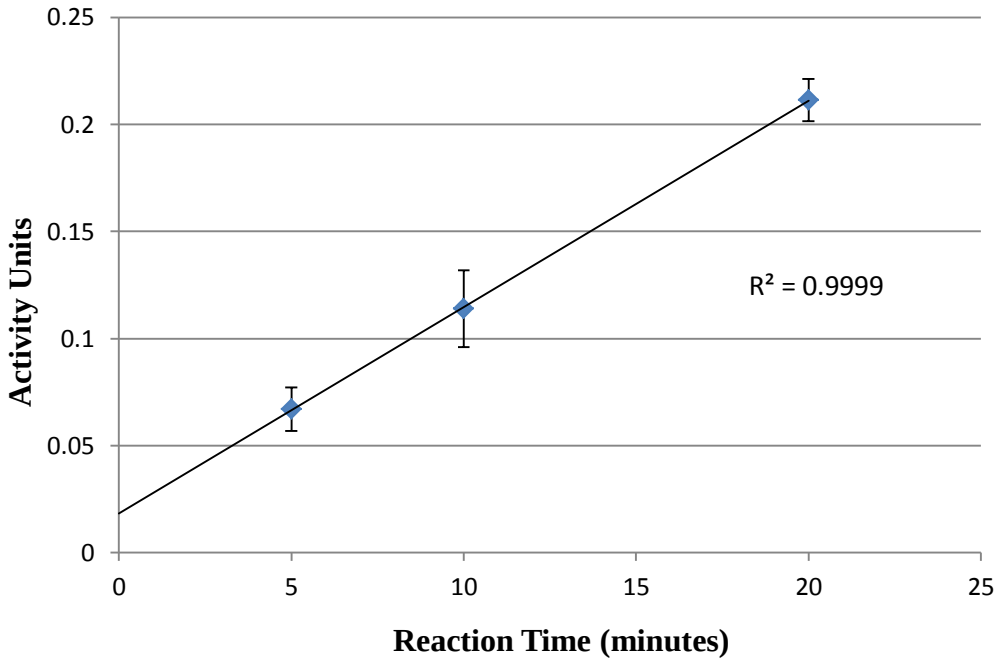

Figure 11. Results for Variation of Incubation Time in the CYP3A4 Model Assay

The final step in developing the CYP3A4 assay prior to the inhibition studies involved testing varying substrate (erythromycin) concentrations. The resulting data should demonstrate a non-linear relationship between reaction rate and substrate concentration, resulting in a rectangular hyperbolic curve indicative of Michaelis-Menten kinetics. The K_m value can be extracted from the plot, giving a relatively ideal substrate concentration to use in the acai berry inhibition study. At such a concentration, 50% of the enzyme is bound to the substrate, creating a reaction environment in which inhibition can be readily observed. Figure 12 shows the results of testing the CYP3A4 reaction with 0.1 – 25 µM of erythromycin. The resulting K_m value of 4.9 µM and V_{max} value of 2.6 x

10^{-2} activity units/mg of protein/minute were obtained from the data. An erythromycin concentration of 10 µM was adopted from this K_m value and used in the acai berry inhibition screening.

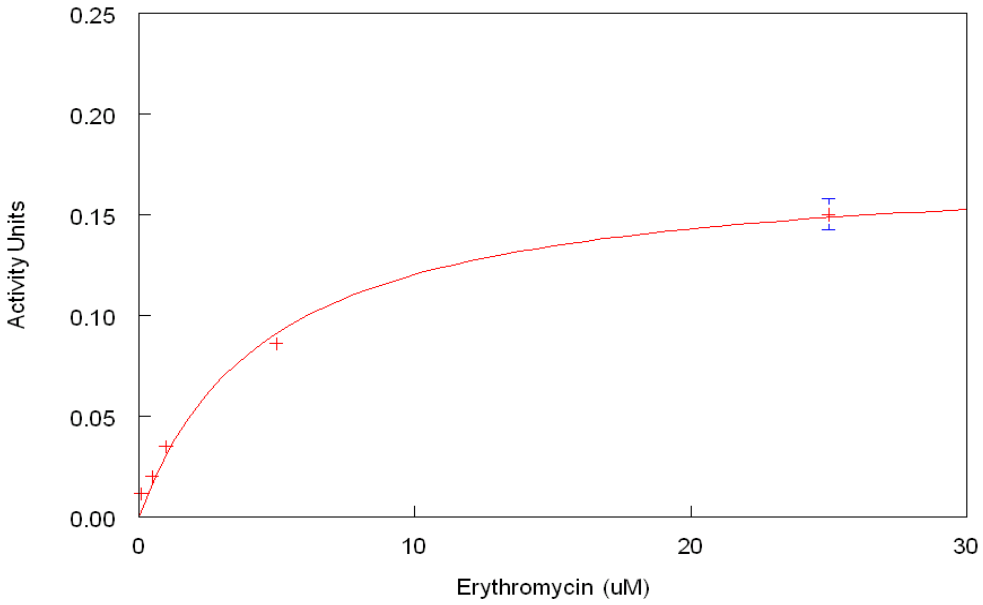

Figure 12. Michaelis-Menten Curve of CYP3A4 Model Erythromycin N-Demethylase.

3.1.2 CYP2D6 Model Assay

The CYP2D6 dextromethorphan O-demethylation reaction was first tested with variable enzyme concentrations and total formaldehyde produced was measured by the Nash assay. The goal of this experiment was to establish linearity between reaction rate and enzyme concentration, as well as selecting an appropriate volume of rat liver microsomes to use in the subsequent CYP2D6 assays. These reactions were carried out in similar conditions described in the Experimental section. Figure 13 illustrates the results of these reactions, which were tested with 15-45 µL of rat liver microsomes. A linear

increase in activity, measured in activity values from the Nash Assay, can be observed in correlation with the increase in microsome concentration. The volume of 15 µL, in order to conserve the rat liver microsome stock solution while still giving adequate activity, was chosen for subsequent CYP2D6 reactions.

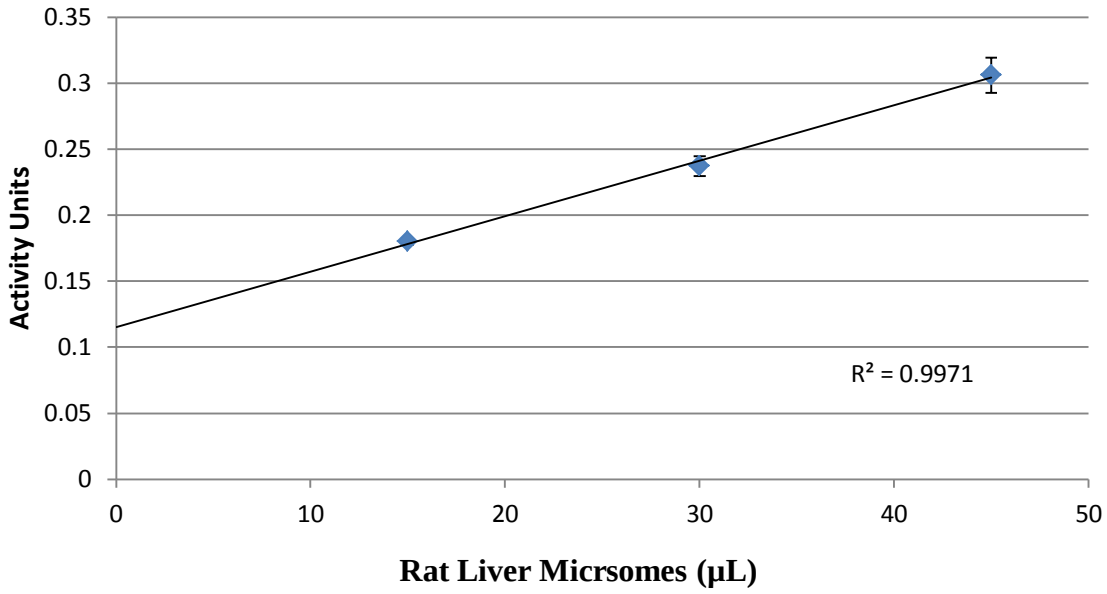

Figure 13. Results for Variation of Microsomal Volume in the CYP2D6 Model Assay.

Additionally, the CYP2D6 reaction was tested with varying reaction times to ensure linearity over the entire course of the reaction. This involved carrying out reactions with 15 µL of microsomes and incubation times that varied from 15-45 minutes, the results of which can be seen in Figure 14. The data indicates a linear increase in production formation in relation to the increase in reaction time. For the acai berry screening, an incubation time of 30 minutes was decided upon for the CYP2D6 assay.

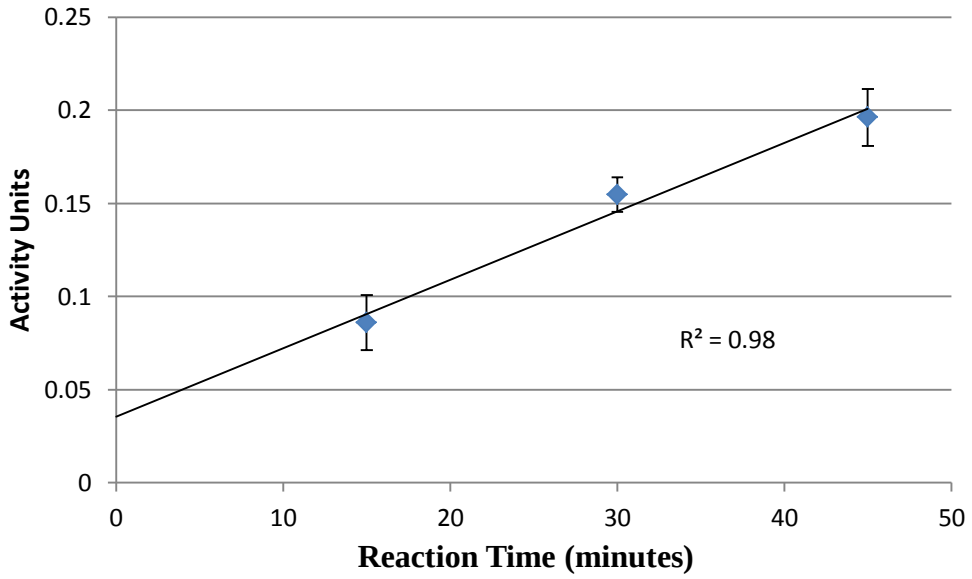

Figure 14. Results for Variation of Incubation Time in the CYP2D6 Model Assay.

Examining the relationship between substrate (dextromethorphan) concentrations and reaction activity was the last step in optimizing the CYP2D6 assay for inhibition study. Dextromethorphan was varied at a range of 0.1 – 50 µM; the results of which are shown in Figure 15. As demonstrated in the graph, activity follows a non-linear relationship indicative of Michaelis-Menten kinetics. Here, the V_{max} of the reaction was determined to be 3.2 x 10^{-2} activity units/mg of protein/minute. A value of 9.2 µM was determined for the K_m of the reaction, and a dextromethorphan concentration of 10 µM was determined to be appropriate for use in the acai berry inhibition screening study.

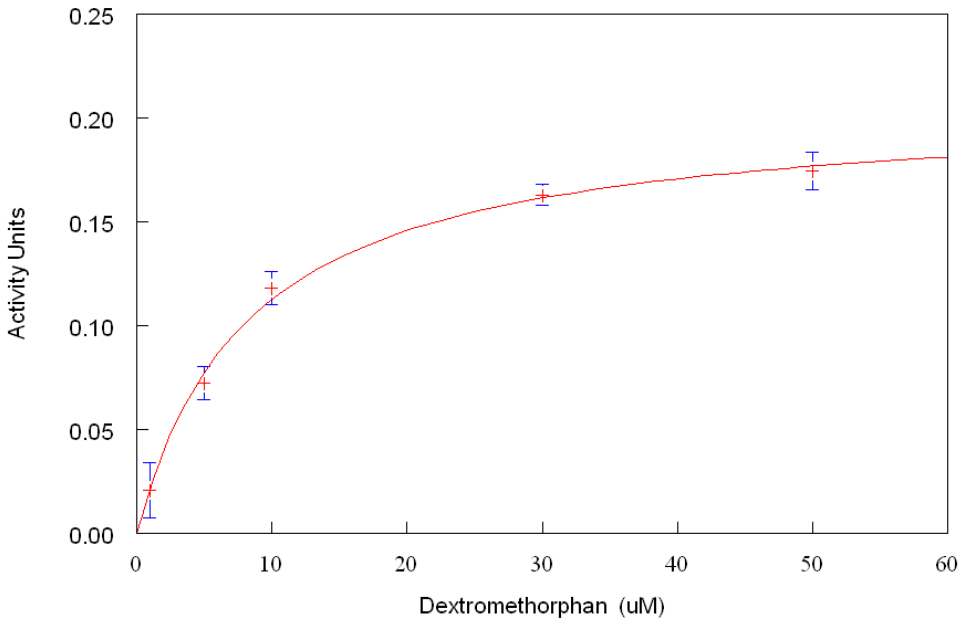

Figure 15. Michaelis-Menten Curve of CYP2D6 Model Dextromethorphan O-Demethylation.

3.1.3 MCOD Assay

Optimization of 7-methoxycoumarin O-demethylase involved testing the assay with variable enzyme concentrations. A linear relationship should be observed between enzyme concentration and product formation in the MCOD reaction. As illustrated in Figure 16, the assay was tested with human S9 fractions at a range of volumes between 1-5 µL, demonstrating linearity in the reaction. For optimization, 3 µL of S9 fraction microsomes were selected based on the adequate amount of observed fluorescence activity, and subsequently used in future MCOD experiments. Also, this small volume was selected to maximize the number of reactions that could be carried out from a single aliquot of human S9 fraction stock solution.

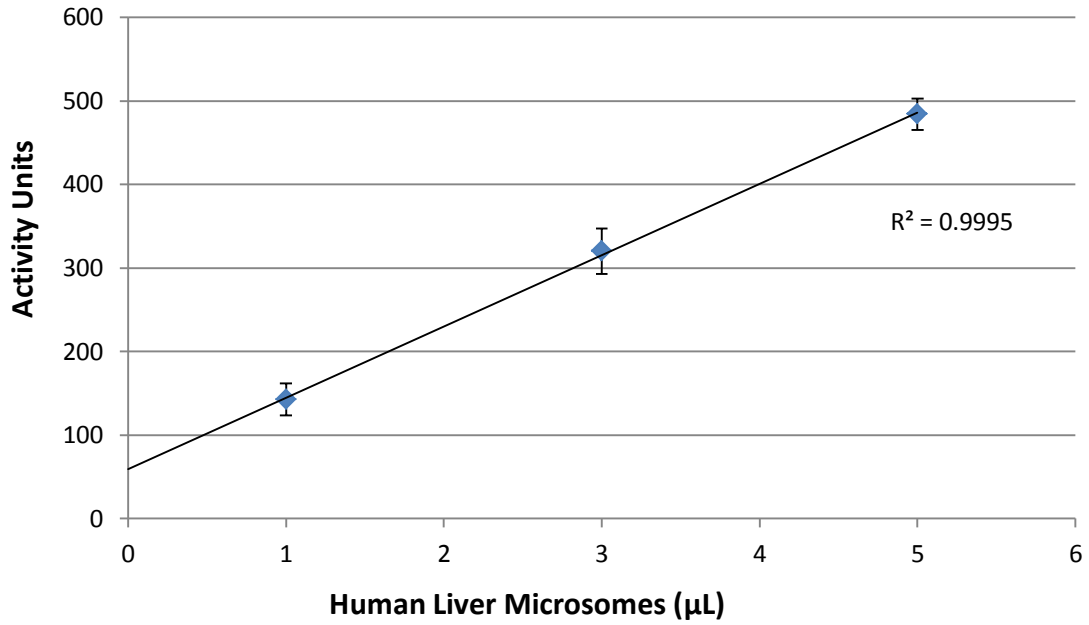

Figure 16. Results for Variation of Microsomal Volume in the MCOD Assay.

Additionally, the MCOD assay was tested with varying reaction times. These reactions were carried out with 3 µL of S9 fraction microsomes and incubation times that varied from 15-60 minutes. In Figure 17, the results of this experiment show that there is a linear increase in enzyme activity in relation to the increase in reaction time. Based on the sufficient amount of activity observed, a reaction incubation time of 45 minutes was selected as the optimal time for MCOD assays during the inhibition studies.

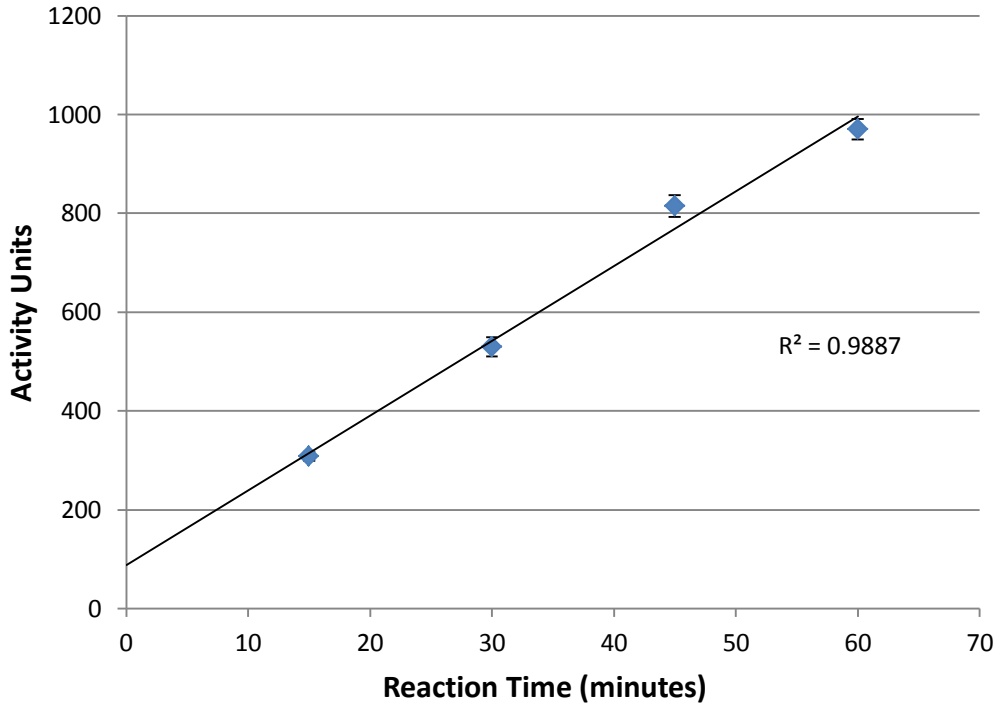

Figure 17. Results for Variation of Incubation Time in the MCOD Assay.

The final step in optimizing the MCOD assay involved examining the relationship between varying concentrations of the substrate (7-methoxycoumarin) and reaction rate. Figure 18 shows the results of this experiment using 25 – 600 µM 7-methoxycoumarin. The results indicate a non-linear relationship indicative of Michaelis-Menten kinetics, with a K_m value of 53 µM and V_{max} of 1.2 x 10^2 activity units/mg of protein/minute in the reaction. Based on the K_m value, a substrate concentration of 50 µM was selected to be used during the inhibition studies on MCOD.

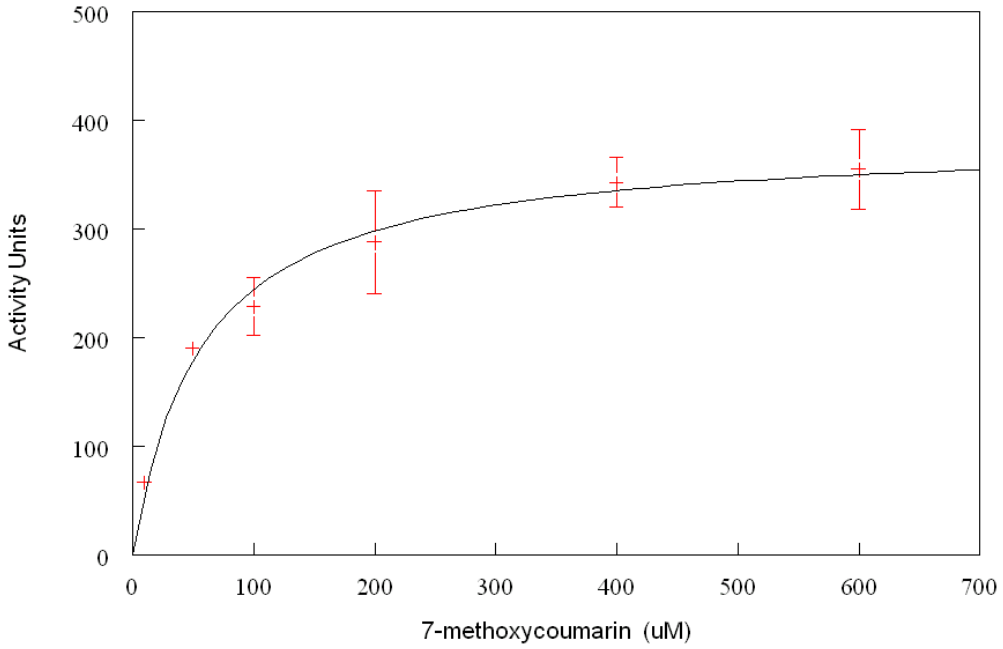

Figure 18. Michaelis-Menten Curve of the 7-Methoxycoumarin O-Demethylation Reaction.

As discussed previously, multiple cytochrome P450 isoforms are responsible for the 7-methoxycoumarin reaction. The initial assumption was CYP2B6 was a major contributor, but that CYP1A2[62]and 2A6[63] could play a role in the metabolism of 7-MC as well. An additional objective was to confirm involvement of specific isoforms using selectively-expressed cytochrome P450 supersomes. Each of the available supersomes (CYP2A6, 1A1, 1A2, 2E1, and 2C8) was tested in control reactions with 50 µM 7-methoxycoumarin, 0.1 M phosphate buffer, 1.0 mM NADPH, and 3 µL of supersomes. The results, shown in Figure 19, displayed observed fluorescence activity indicative of 7-hydroxycoumarin formation. From these results, it can be implied that in addition to 2B6. CYP2A6, 1A2, and 2E1 demonstrate prominent 7-methoxycoumarin O-demethylation activity.

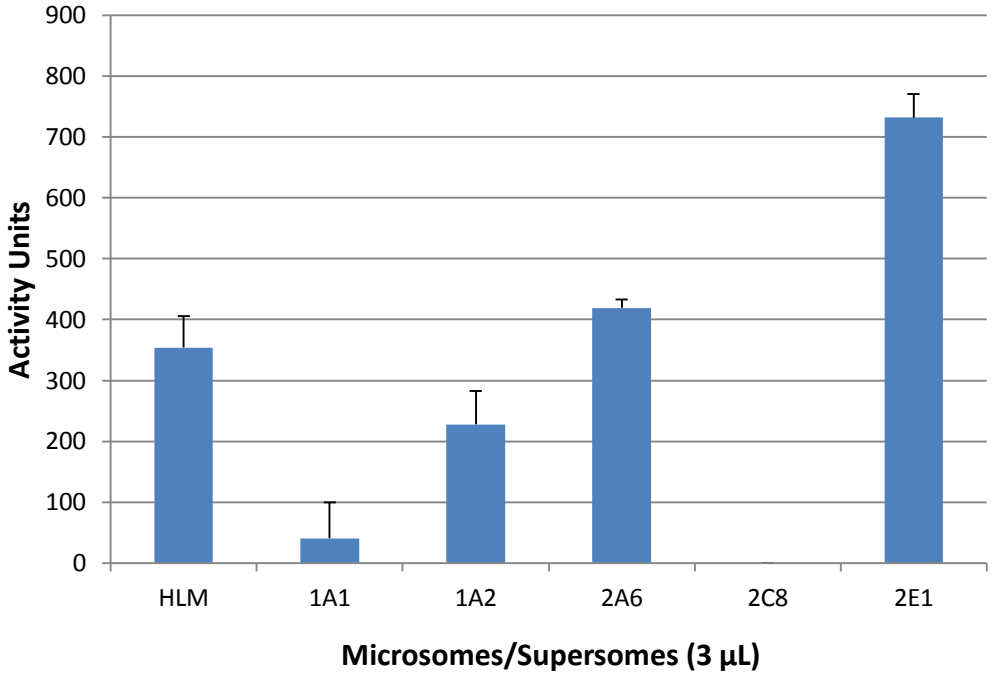

Figure 19. Results for Screening of Several Cytochrome P450 Isoform-Specific Supersomes for MCOD Activity.

3.2.0 Inhibition-Directed Fractionation of Acai Berry

The initial fractionation, summarized in Scheme 1, produced four crude samples for bioactivity testing. These initial fractions were screened for inhibition in the rat cytochrome P450 3A4, 2D6, and human MCOD assays, as described in the Materials and Methods section. The results were as follows:

3.2.1 Crude Acai Berry Fractions

The initial acai berry fractions were tested for bioactivity with the CYP3A4 assay. The objective of this experiment was to observe reduction in CYP3A4 activity from each crude fraction in the reaction mixture. Each assay was performed with 10 µM substrate, 1.1 mg/mL rat liver microsomes, and incubated for 30 minutes, as established in section

3.1.1. The fractions were tested individually at a final reaction concentration of 200 µg/mL. This high concentration was used in order to catch high potency, low abundance inhibitors that may be present. The results of this experiment, as seen in Figure 21, are presented as percentage of activity in the acai-treated reactions versus the control. The aqueous fraction showed 100.1 ± 3.9 % activity, the butanol fraction showed 96.0 ± 1.2 %, the chloroform fraction showed 111.0 ± 0.5 %, and the hexane fraction showed 107.5 ± 0.5 activity. No remarkable reduction in CYP3A4 activity was observed for any of these crude fractions, and further fractionation based on CYP3A4 inhibition was not pursued. Such results indicate that multiple extracts of the acai berry do not interfere with CYP3A4 metabolism. In particular, the butanol fraction was expected to be rich in anthocyanins, a class of pigmented flavonoids that have been shown to be only weak inhibitors of human CYP3A4[37], which is consistent with the lack of inhibition observed in the current study using the butanol extract. While there still may be the possibility that a CYP3A4 inhibitor could be present in other extracts, it is doubtful they pose any pharmacokinetic significance due to their extremely low concentrations.

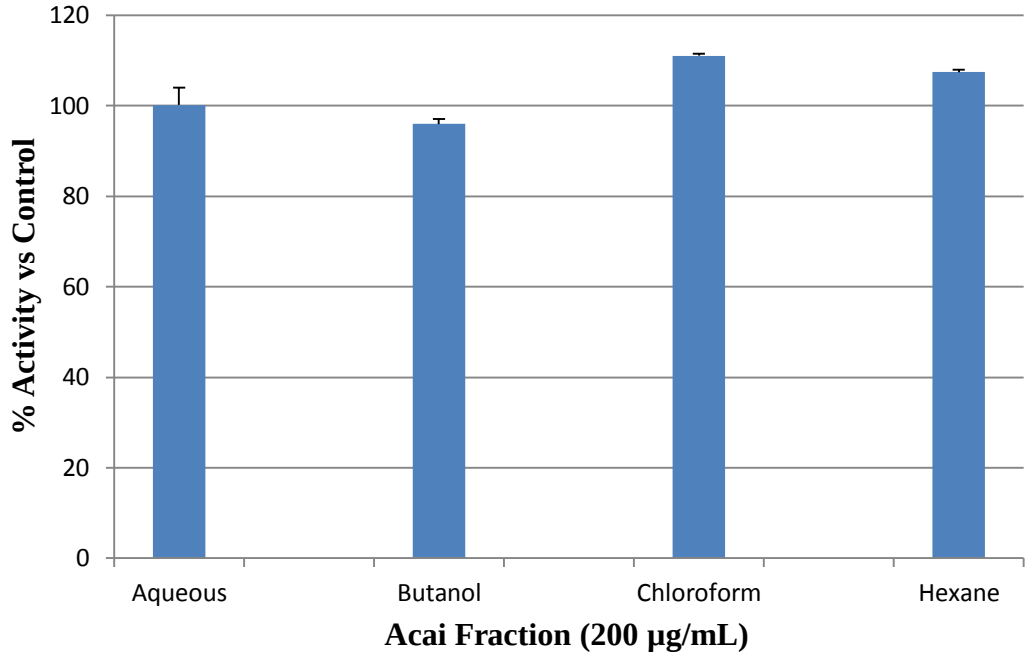

Figure 20. Results for the Screening of the Crude Fractions for CYP3A4 Inhibition.

The crude acai berry fractions were tested with the CYP2D6 assay. Similar to the previous experiment, the goal of this experiment was to determine bioactivity of each initial fraction by observing loss of CYP2D6 activity. The assays were carried out under conditions described in section 3.2.2, with 10 µM substrate, 1.1 mg/mL rat liver microsomes, and incubated for 30 minutes. The results of these assays, as seen in Figure 21, are reported as percentage of activity in the reactions containing acai fraction versus the control. The aqueous fraction showed a 96.7 ± 0.6 % activity; butanol fraction showed 79.7 ± 1.4 %; chloroform fraction showed 110.3 ± 1.9 %; hexane fraction showed 104.9 ± 0.3 % activity. Although the anthocyanin-rich butanol fraction did show modest inhibition, these compounds are classified as weak inhibitors of CYP2D6 as well[65]. Given this knowledge of CYP2D6, along with the lack of inhibition observed at

200 µg/mL, it is unlikely that there is any physiologically significant inhibition of CYP2D6 by acai products. Thus for this assay, no further fractionation was carried out.

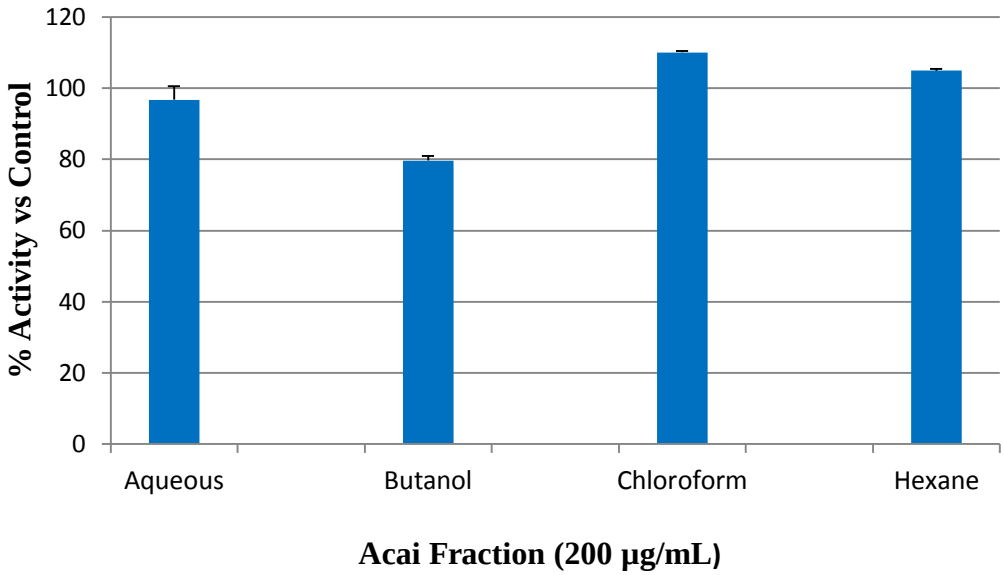

Figure 21. Results for the Screening of the Crude Fractions for CYP2D6 Inhibition.

The crude acai fractions were next tested for inhibition of 7-methoxycoumarin O-demethylation activity. Once again, each crude fraction was screened individually at a final reaction concentration of 200 µg/mL. For this experiment, reactions were carried out under optimal conditions established in section 3.1.3, with 50 µM substrate, 0.35 mg/mL S9 microsomes, and incubated for 45 minutes. The results of these assays, as seen in Figure 22, are presented as percentage of activity in the presence of the acai fractions relative to the control. Once again, for the purpose of clarification, "active fractions" are defined as those that result in a substantial reduction in MCOD activity. Reactions carried out in the presence of 200 µg/mL of the dried aqueous extract showed 80.0 ± 5.0 % activity, while the butanol extract yielded 83.7 ± 1.9 % activity. The chloroform extract,

on the other hand, reduced the activity of MCOD to 5.3 ± 0.3 % of the control, while the hexane extract resulted in a more modest reduction to 43.0 ± 8.4 % activity. Since the chloroform extract showed the most remarkable inhibition of MCOD activity, it was selected for further fractionation. The hexane extract, although somewhat inhibitory, was not further fractionated.

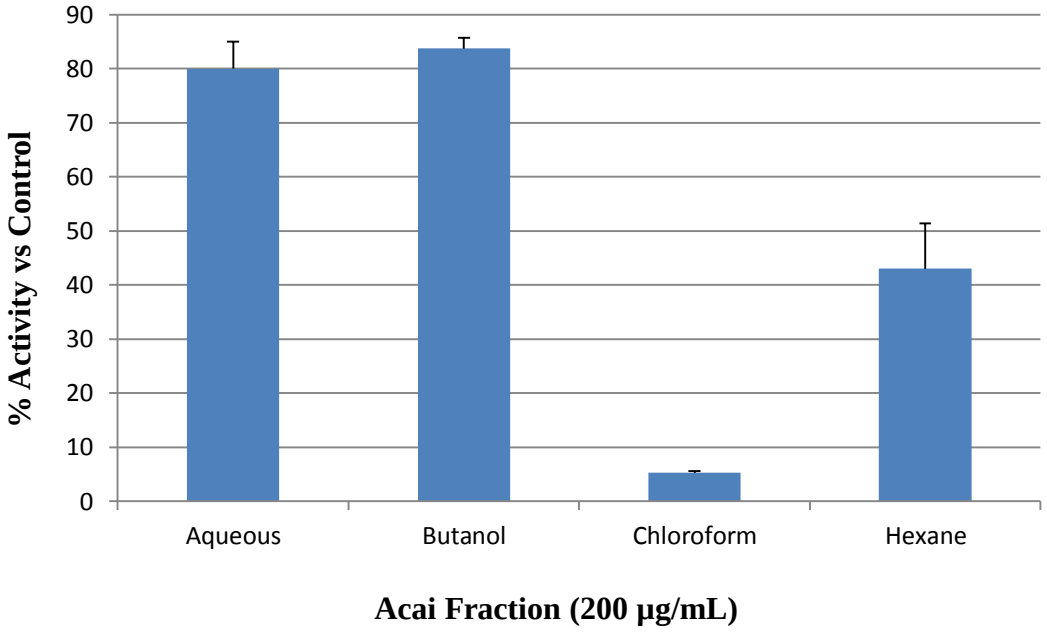

Figure 22. Results from the Screening of the Crude Fractions for MCOD Inhibition.

3.2.2 Generation 1 (34 Series)

Fractionation of the chloroform extract resulted in the creation of ten samples designated as the 34 series, as illustrated in Scheme 3. These fractions were tested in the MCOD reaction along with the parent chloroform fraction. The concentration of each extract in these reactions was lowered to 50 µg/mL in order to distinguish which fractions contained the more potent inhibitors. The results of this screening are shown in Figure 23,

and are reported as percentage activity in the presence of extract, relative to controls. Reactions containing the parent fraction showed 24.1 ± 6.4 % activity, 34-01 showed 81.8 ± 7.9 % activity, 34-02 showed 65.4 ± 5.0 % activity, 34-03 showed 79.1 ± 5.2 % activity, 34-04 showed 84.8 ± 6.5 % activity, 34-05 showed 60.6 ± 0.5 % activity, 34-06 showed 59.7 ± 6.4 % activity, 34-07 showed 40.3 ± 3.3 % activity, 34-08 showed 35.1 ± 5.1 % activity, 34-09 showed 59.7 ± 5.6 % activity, and 34-10 showed 49.3 ± 1.9 % activity. It should be noted that there was an expectation that many fractions would show some degree inhibition. CYP450 enzymes have broad substrate selectivity, which is an important property in relation to its function of detoxification. The complexity of natural product extracts, including the acai berry, leads to a high potential for inhibition of CYP450 enzymes by multiple components. The scope of this portion of the study is to identify those fractions which have the strongest potential for inhibition, particularly when compared to their parent fraction. For this experiment, 34-08 fraction was chosen for further fractionation due to its pronounced inhibition of MCOD. The other fractions were not further investigated.

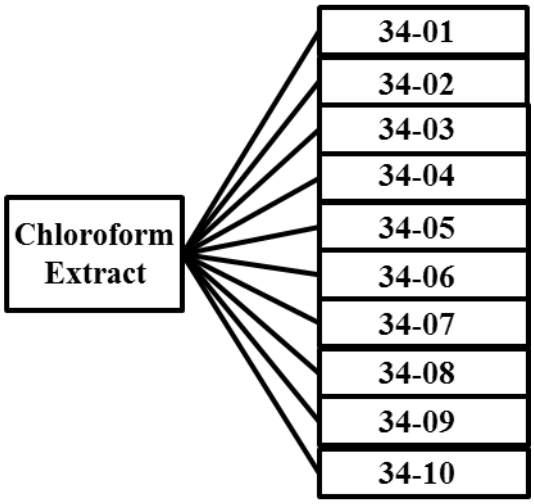

Scheme 3. Generation of the 34 Series of Fractions.

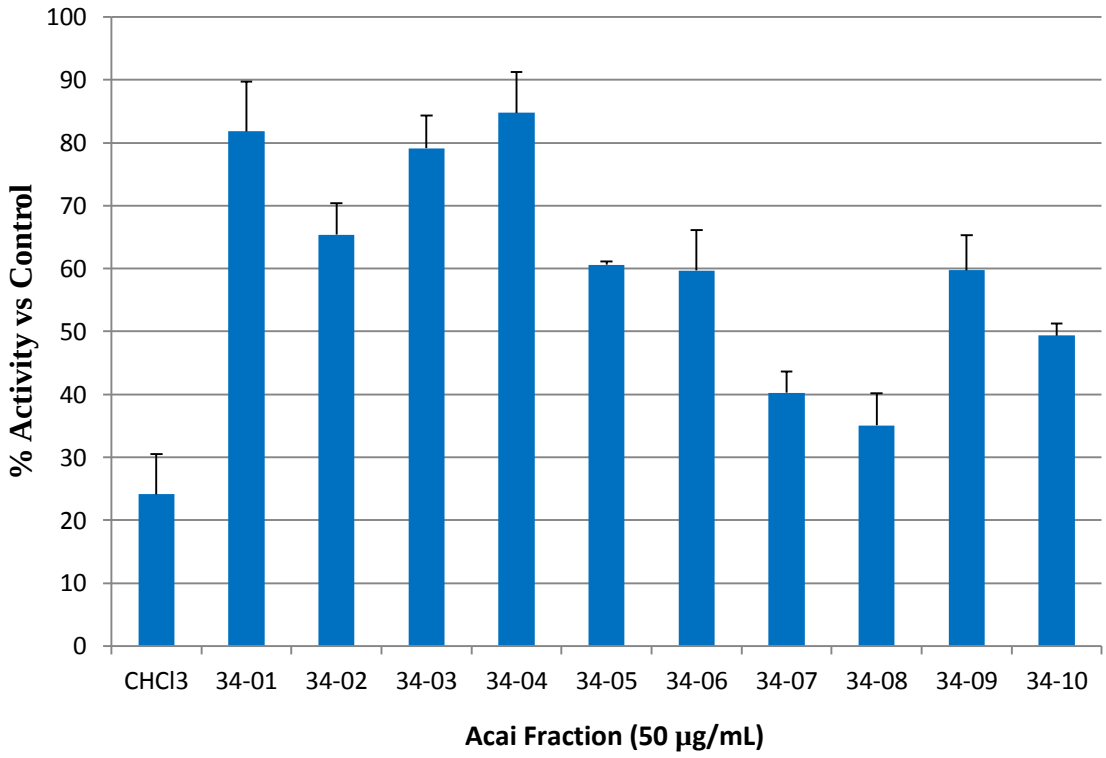

Figure 23. Results for the Screening of the 34 Series Fractions. These were screened along with the parent chloroform fraction at 50 µg/mL reaction concentration.

3.2.3 Generation 2 (38 Series)

The 34-08 fraction was partitioned into eight samples, the 38 series, as seen in Scheme 4. In this experiment, each of these eight samples, along with the parent fraction, were tested in the 7-methoxycouamrin O-demethylation reaction at a concentration of 50 µg/mL. As before, the results of this screening are reported as percentage of activity relative to the control reaction (Figure 24). At this dose, the parent 34-08 sample reduced activity to 28.8 ± 6.1 %, 38-01 reduced activity to 36.1 ± 2.3 %, 38-02 resulted in 26.4 ± 3.0 % activity, 38-03 resulted in 44.5 ± 5.1 % activity, 38-04 resulted in 66.7 ± 14.2 % activity, 38-05 resulted in 49.9 ± 7.9 % activity, 38-06 resulted in 24.8 ± 9.7 % activity, 38-07 resulted in 30.2 ± 4.8 % activity, and 38-08 resulted in the most substantial reduction in activity with only 11.3 ± 1.2 % remaining. Once again, a significant number of fractions showed varying degrees of low to moderate inhibition. From this experiment, 38-02, 38-06, and 38-08 showed remarkable inhibition of the MCOD reaction. Given the multitude of bioactive fractions, the next generation bifurcated into two offspring series. 38-02 was partitioned into five fractions, referred to as the 62 series. 38-06 and 38-08, due to limited sample availability, were pooled together with 38-07 and subsequently partitioned into the 86 series, producing seven fractions.

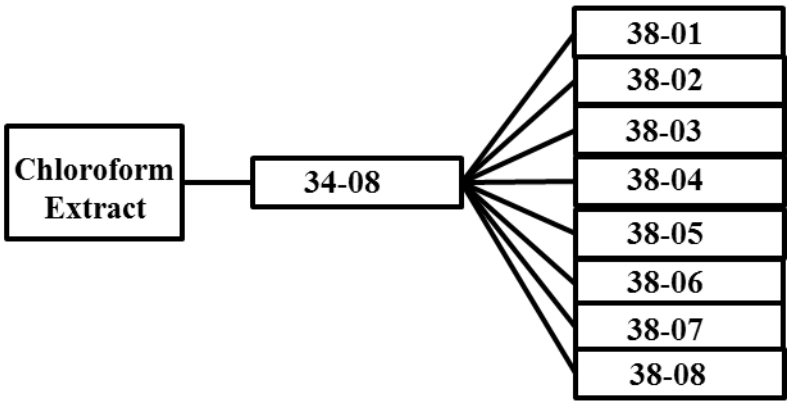

Scheme 4. Generation of the 38 Series of Fractions

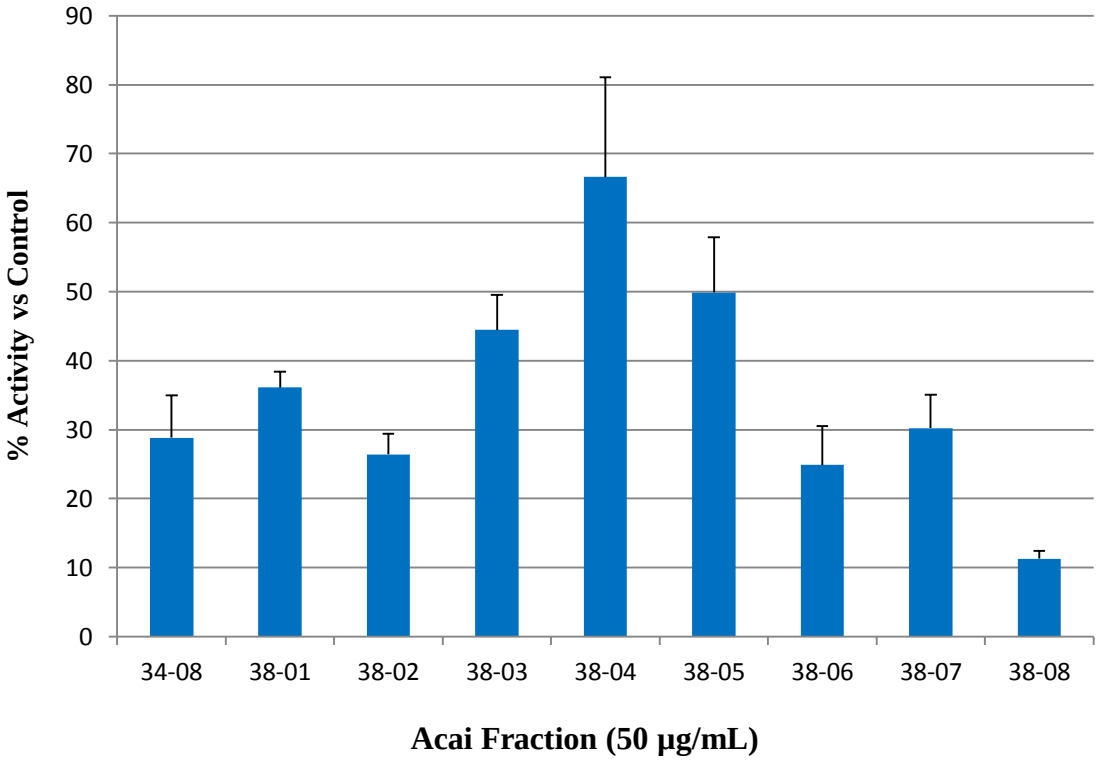

Figure 24. Results for the Screening of the 38 Series Fractions. These fractions were screened along with the parent 34-08 fraction at 50 µg/mL reaction concentration.

3.2.4 Generation 3 (62 and 86 Series)

38-02 was partitioned into five fractions designated as the 62 series, as seen in Scheme 5. These fractions were tested in the MCOD assay for inhibition along with the parent fraction. The fraction concentration in the reactions was lowered to 25 µg/mL in order to distinguish which fractions contained the more potent inhibitors. The results, shown in Figure 25, are once again reported as percent activity relative to the control. The parent fraction reported activity at 58.1 ± 1.7 %, 62-01 at 73.7 ± 2.2 % activity, 62-02 at 53.9 ± 8.9 % activity, 62-03 at 51.3 ± 9.5 % activity, 62-04 at 61.9 ± 10.8 % activity, and 62-05 at 100.9 ± 12.3 % activity. The 62-02 fraction was selected to be furthered studied and fractionated into the 78 series, along with the 62-03 fraction, which was fractionated into the 82 series. The other fractions were not further investigated.

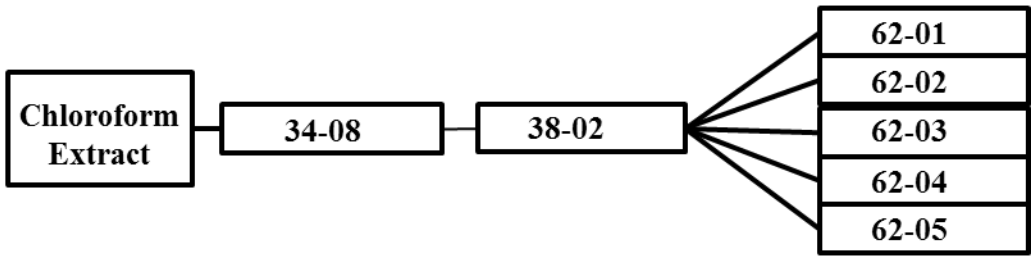

Scheme 5. Generation of the 62 Series of Fractions.

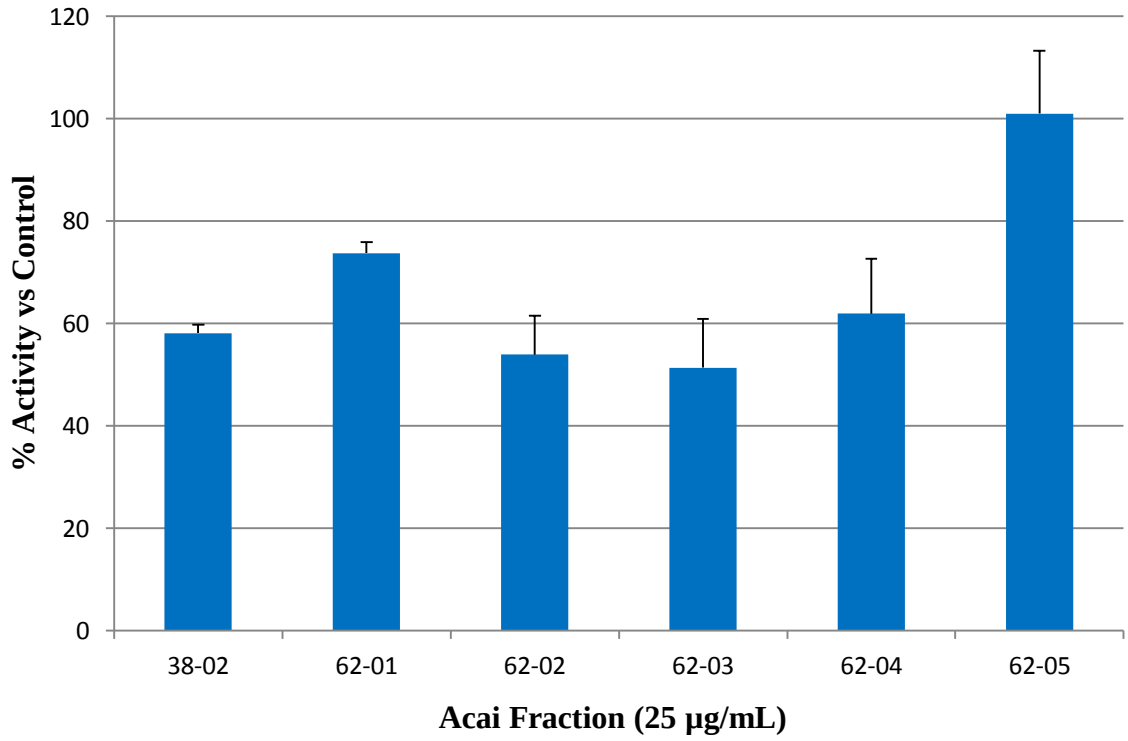

Figure 25. Results for the Screening of the 62 Series Fractions. These fractions were tested along with the parent 38-02 fraction at 25 µg/mL reaction concentration

As previously stated, the 86 series contains seven fractions, whose starting material (defined as 86-SM) are the amalgamation of 38-06, 38-07, and 38-08 fractions from the previous generation. Each fraction, along with starting material, was tested in the MCOD reaction at 50 µg/mL. The results of this screening are reported in Figure 26, showing the percentage of observed activity in acai-treated reactions relative to control. 86-SM showed 48.5 ± 7.6% activity, 86-01 showed 90.8 ± 9.6% activity, 86-02 showed 65.1 ± 9.3% activity, 86-03 showed 55.8 ± 8.9% activity, 86-04 showed 54.2 ± 6.8% activity, 86-05 showed 47.6 ± 5.3% activity, 86-06 showed 42.1 ± 5.2% activity, and 86-07 showed 50.0 ± 11.1 % activity. Several fractions, including 86-05, 06, and 07 showed remarkable inhibition when compared to the starting material. However, further investigation into the composition of these fractions have yet to be pursued at this time.

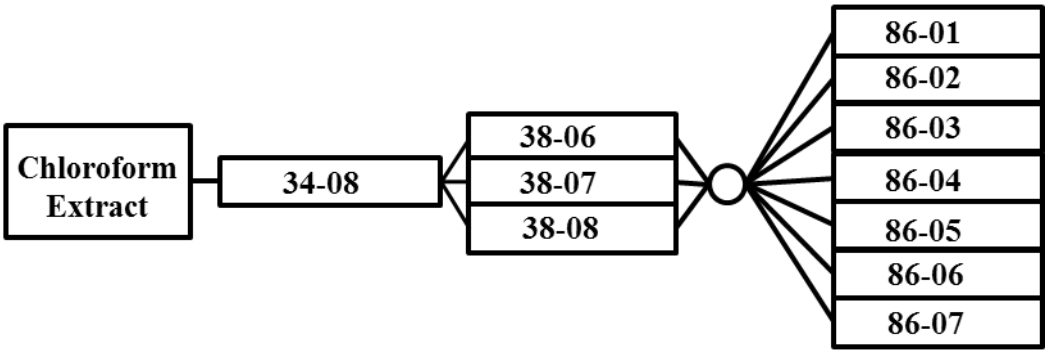

Scheme 6. Generation of the 86 Series of Fractions.

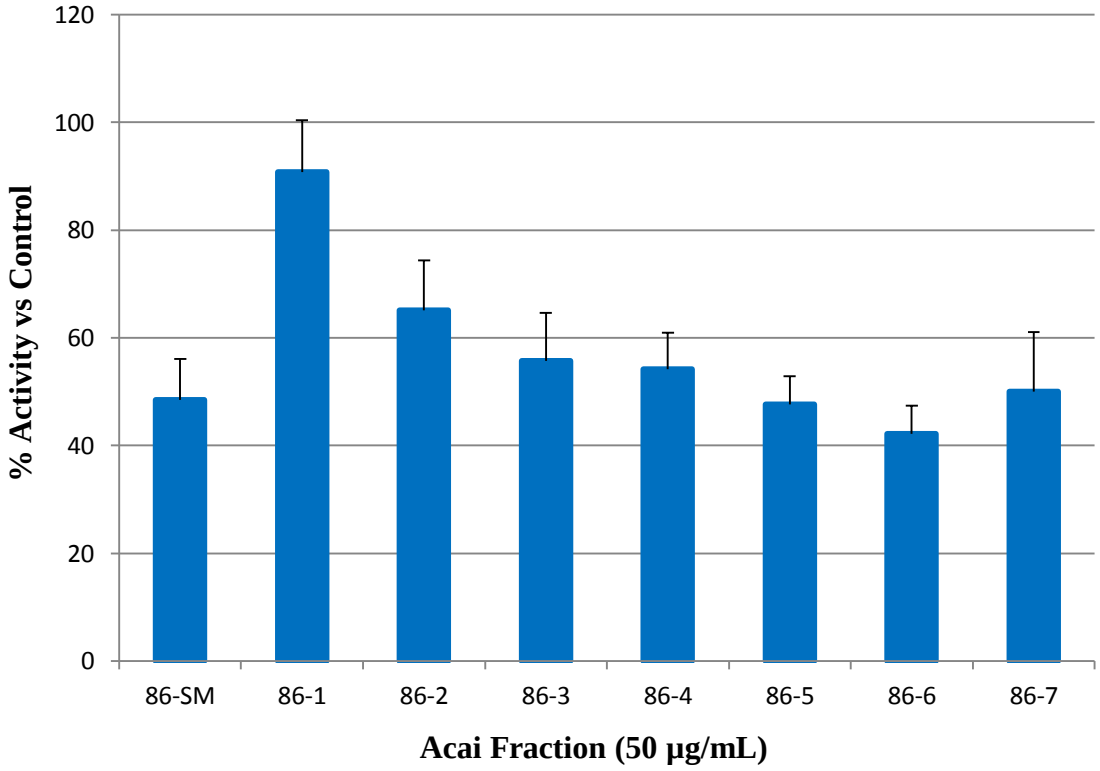

Figure 26. Results for the Screening of the 86 Series Fractions. The starting material, 86-SM, is comprised of the 38-06, 38-07, and 38-08 pooled together. These fractions were screened at a reaction concentration of 50 µg/mL.

3.2.5 Generation 4 (78 and 82 Series)

The 62-02 fraction was investigated first, and resulted in the creation of eight fractions designated as the 78 series. These fractions were tested in the MCOD reaction, along with the parent fraction, at 25 µg/mL. The results of this screening are shown in Figure 27, and are reported as percentage of activity in the acai-treated reactions versus the control. The parent fraction (62-02) produced activity of 28.3 ± 13.1 %, 78-A gave 64.0 ± 2.1 % activity, 78-B gave 90.3 ± 20.5 % activity, 78-C gave 50.8 ± 4.3 % activity, 78-D gave 25.8 ± 3.8 % activity, 78-E gave 60.1 ± 7.7 % activity, 78-F gave 68.6 ± 4.7 % activity, 78-G gave 42.5 ± 7.8 % activity, and 78-H gave 52.7 ± 11.6 % activity. The 78-D fraction, showing 74.2 % inhibition of 7-methoxycoumarin metabolism, was further investigated in order to determine its inhibition constant (K_i) and mode of inhibition.

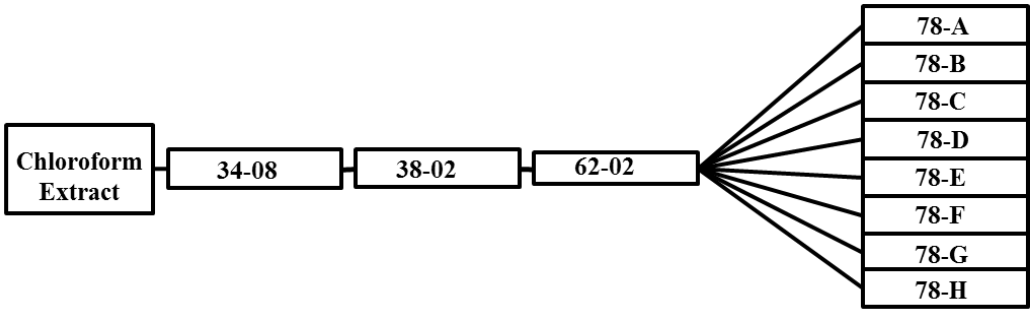

Scheme 7. Generation of the 78 Series of Fractions.

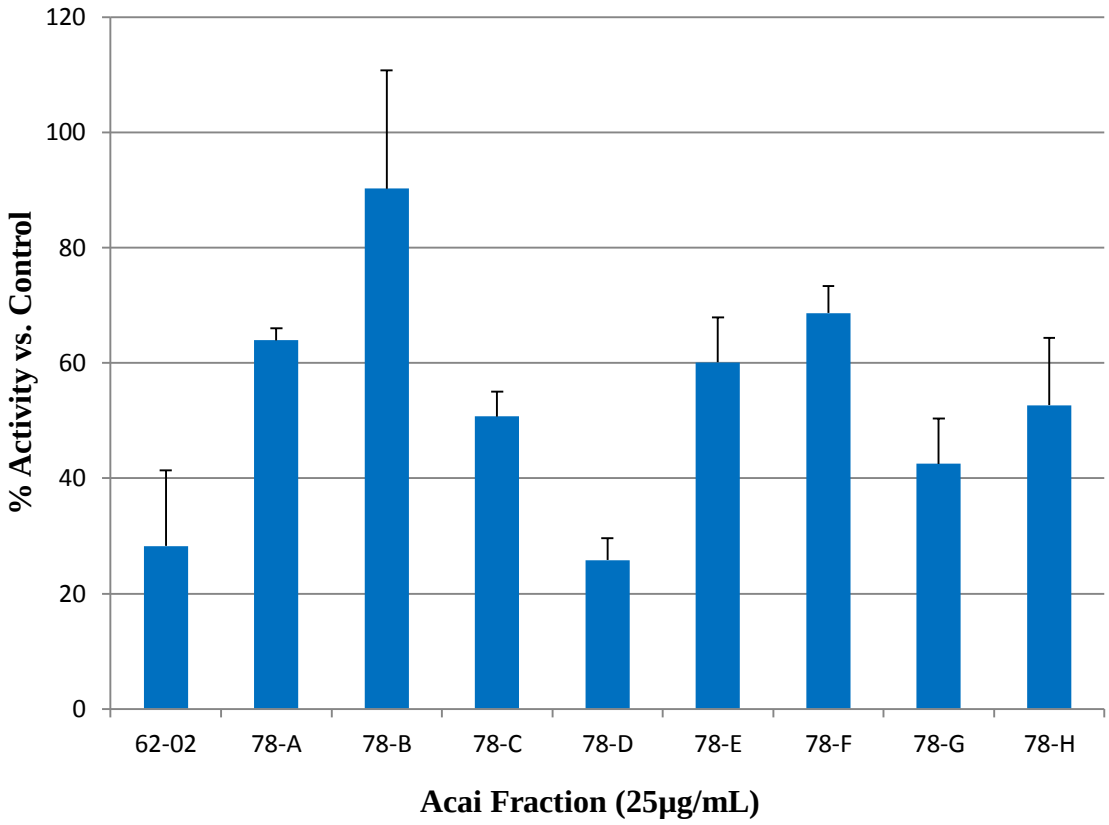

Figure 27. Results for the Screening of the 78 Series Fractions. These fractions were tested along with the parent 62-02 fraction at 25 µg/mL reaction concentration.

The last series of fractionations was performed on 62-03, and resulted in the creation of seven fractions designated as the 82 series. These fractions were tested in the MCOD reaction, along with the parent fraction, at 25 µg/mL. The results of this screening are shown in Figure 28, and are reported as percentage of activity in the acai-treated reactions versus the control. The parent fraction (62-03) reported activity of 23.3 ± 6.1 %, 82-A reported 47.0 ± 0.7 % activity, 82-B reported 10.8 ± 3.9 % activity, 82-C reported 11.7 ± 3.4 % activity, 82-D reported 13.6 ± 7.3 % activity, 82-E reported 43.9 ± 7.3 % activity, 82-F reported 23.1 ± 3.6 % activity, an 82-G reported 21.4 ± 0.4 % activity. Based on this analysis, the 82-B, 82-C, and 82-D fractions were determined to be the most potent, due to their inhibition relative to the starting material (62-03). Both 82-C and 82-D underwent further analysis in order to characterize their inhibition type and determine their K_i value. Supply of the 82-B fraction had been diminished at this time in the study, and was unable to be analyzed.

Scheme 8. Generation of the 82 Series of Fractions.

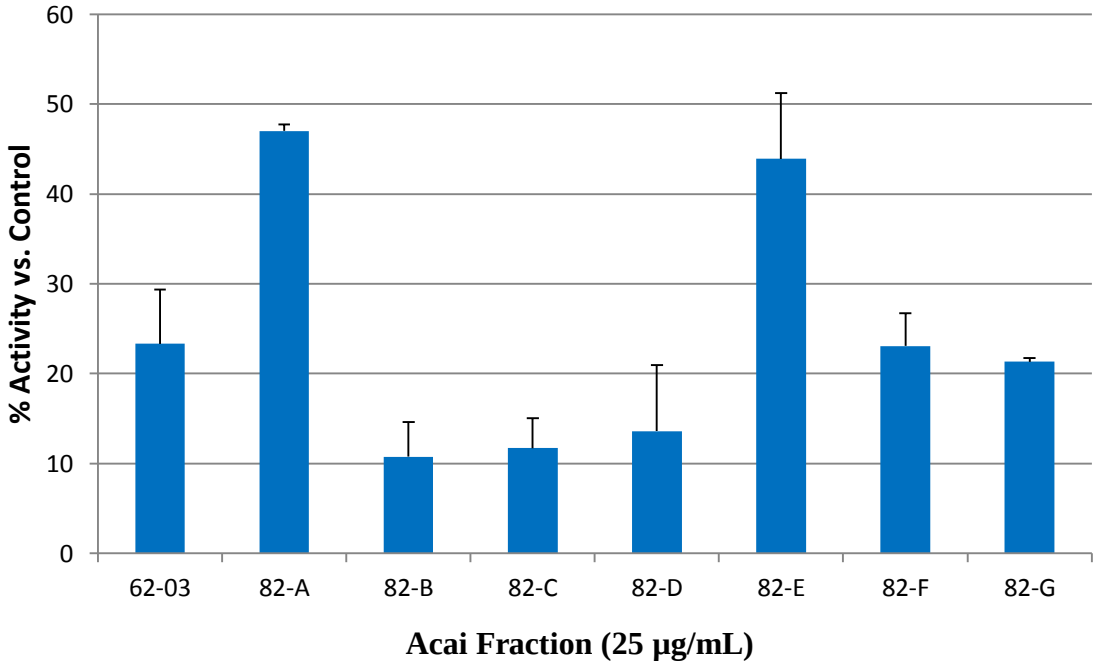

Figure 28. Results for the Screening of the 82 Series Fractions. This series, along with the parent 62-03 fraction, was tested at 25 µg/mL reaction concentration.

3.2.6 Characterization of Later-Stage Fractions

Three later-stage fractions were selected for further analysis based on their high relative inhibition at 25 µg/mL. Each fraction underwent an experiment favoring Michaelis-Menten conditions; examining the MCOD reaction at variable 7-methoxycoumarin concentration in the presence and absence of the fraction of interest. This type of experiment can give both qualitative and quantitative analysis of these fractions, both in terms of their inhibition type and K_i value, respectively.

When a compound inhibits an enzyme, it will induce a change in either the V_{max} and/or K_m of the substrate reaction. By observing the apparent K_m (K_m^{app}) and V_{max} (V_{max}^{app}) of the inhibited reaction, one can determine the type of inhibition (competitive, non-competitive, and uncompetitive) and K_i of the inhibitor. K_i is a dissociation constant that is defined as the concentration of compound needed to induce inhibition.

78-D, which initially showed 74.2 % reduction of MCOD activity at 25 µg/mL, was the first to undergo analysis. The MCOD reaction was carried out with 5-400 µM substrate concentration in the presence of 25 µg/mL of 78-D. These results were compared to a standard curve generated from MCOD assay under normal conditions. Results from these two reaction conditions were plotted, as seen on Figure 29. The V_{max} of the reaction was greatly reduced, dropping from 7.76×10^4 activity units/mg of protein/minute to a V_{max}^{app} of 3.78×10^4 activity units/mg of protein/minute in the presence of 78-D. The K_m values of the reaction stayed in comparable ranges, with K_m at 28.6 µM and K_m^{app} at 23.4 µM. Non-competitive inhibition, in which the V_{max} is reduced while the K_m remains the same, is implicated in this analysis. This type of inhibition is

characterized by the binding of the inhibitor onto an allosteric site on the enzyme. As seen in Equation 2, the K_i of a non-completive inhibitor is calculated based on the change in V_{max}. Using this equation, the K_i of 78-D was determined to be 24 µg/mL.

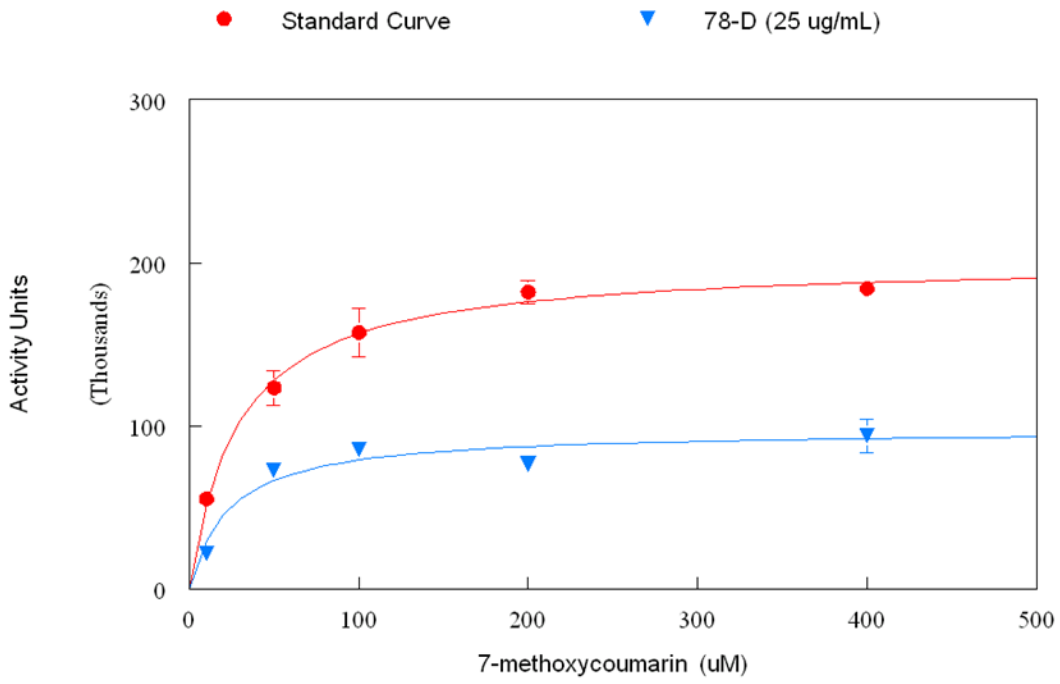

Figure 29. Michaelis-Menten Curves for MCOD in Presence of 78-D.

$$V_{max}/ V_{max}^{app} = 1 + [I]/K_i$$

Equation 2. Equation for Calculating K_i of Non-Competitive Inhibitors.

Additionally, examination undertaken by the Oberlies Group revealed that the contents of the 78-D fraction contained a single compound. Based on an LC/MS and NMR profile, the primary compound in 78-D was estimated to be 1-9-hexadecenoate (328.26 amu), an unsaturated fatty acid seen in Figure 30. Since this fraction was tested at

25 µg/mL, the approximate concentration of the fatty acid in the reaction was 76 µM. The K_i value of 78-D, based on this concentration, is calculated to be 73 µM.

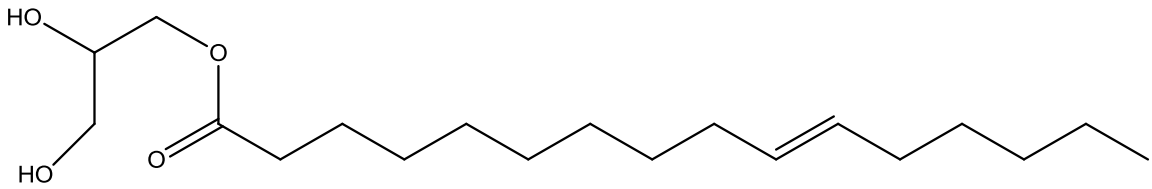

Figure 30. Proposed Structure of Major Constituent of 78-D.

Both 82-C and 82-D underwent the same type of Michaelis-Menten analysis as described above. The MCOD assay, with substrate concentrations ranging from 5-400 µM, was tested in the presence and absence of each fraction at 25 µg/mL. The results, seen in Figure 31, show a marked decrease in the V_{max} and K_m when either fraction is present. The standard curve gave a V_{max} of 7.94×10^4 activity units/mg of protein/minute and a K_m of 84.9 µM. With the 82-C fraction present, the V_{max}^{app} was 3.54×10^4 activity units/mg of protein/minute and the K_m^{app} was 31.8 µM. In the presence of 82-D, the V_{max}^{app} was 4.44×10^4 activity units/mg of protein/minute while the K_m^{app} was 40.4 µM. Based on the decrease in both the V_{max} and K_m of the MCOD assay, these fractions show uncompetitive-type inhibition. Since uncompetitive inhibition affects both the V_{max} and K_m, the K_i can be calculated using either equation in Equation 3. Using these equations, the K_i ranged between 15-20 µg/mL for 82-C and 23-32 µg/m for 82-D.

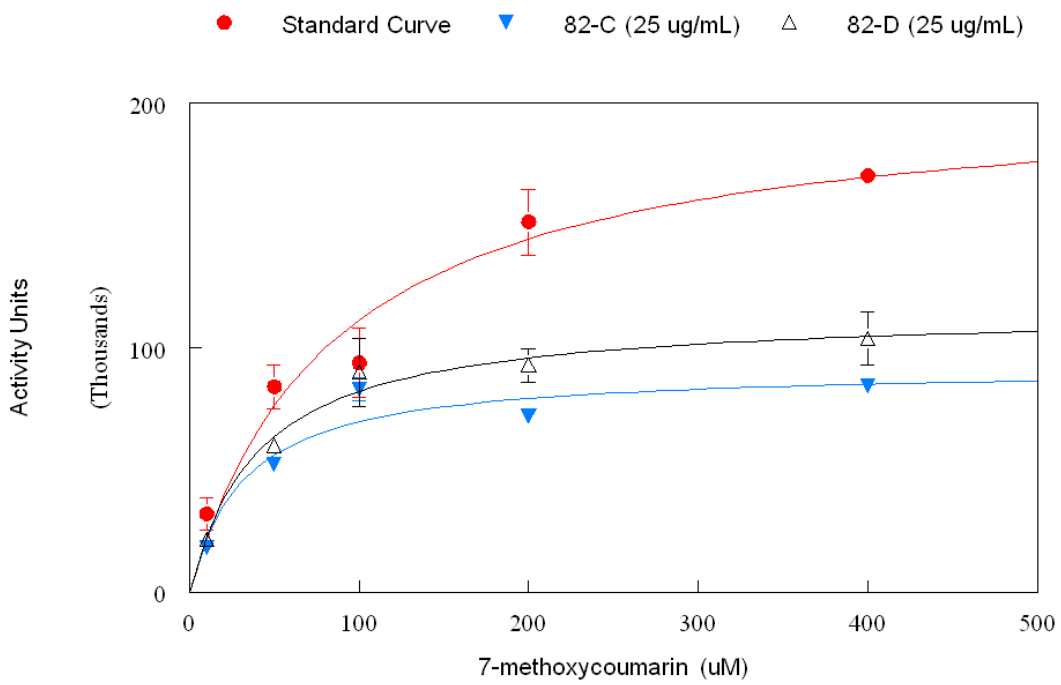

Figure 31. Michaelis-Menten Curves for MCOD in Presence of 82-C and 82-D.

$$V_{max}/\ V_{max}^{app} = 1 + [I]/K_i \qquad K_m/\ K_m^{app} = 1 + [I]/K_i$$

Equation 3. Equations for Calculating K_i for Uncompetitive Inhibitors.

K_i values offer insight into the inhibitory effects of natural products. When examining K_i, lower values indicate stronger inhibition against higher values. Historically, compounds with K_i values < 10 µM are considered strong inhibitors, and are more likely to be linked to herbal-drug interactions[66]. Bergamottin, a strong CYP3A4-inhibitor found in grapefruit juice, was shown to have a K_i as low as 7.7 µM[67]. The 78-D fraction has a K_i of 73 µM, a ten-fold increase when compared to bergamottin. 78-D is similar to the reported K_i value of curcumin (76 µM), a considerably weak inhibitor of the 7-pentoxyresorufuin O-dealkyation assay[68]. Additionally, the K_i values of 82-C (15-

20 µg/mL) and 82-D (23-32 µg/mL) can be compared to a similar study, where ginkgo biloba extracts showed inhibition of human CYP2C9 at a K_i of 14.8 µg/mL[69]. While these findings demonstrated potential of herbal-drug interactions, subsequent *in vivo* studies showed that ginkgo biloba had no effect on the pharmacokinetics of several CYP2C9 probes[70,71]. Such comparisons give indication that these later-stage acai berry fractions, while demonstration remarkable *in vitro* inhibition, are not likely to have an observable effect on *in vivo* drug metabolism.

CHAPTER IV

CONCLUSIONS

The crude acai berry fractions yielded no remarkable inhibition of both the erythromycin N-demethylation (CYP3A4) and dextromethorphan O-demethylation (CYP2D6) reactions. It is important to uncover possible interactions with these isoforms, given the pharmacological importance these enzymes exhibit. These results are further rationalized by the lack of inhibition observed by the butanol fraction. As previously discussed, anthocyanins are a major class of constituents in the acai berry and reside in the butanol extract. Dreiseitel et. al. had previously found these compounds to be weak inhibitors of both CYP3A4[37] and 2D6[65], which corresponds to the results of this study. Additionally, the peak serum levels of anthocyanins were estimated to be 1.1-2.0 ng/mL[36]. Given that the crude fractions were tested at 200 µg/mL, it is unlikely that the concentration of anthocyanins in the acai berry would have any pharamcokinetic impact on these enzymes. Thus, the results of this *in vitro* study imply that the acai berry does not interact with the metabolic activity of cytochrome P450 3A4 and 2D6.

For the 7-methoxycoumarin O-demethylation reaction, the chloroform extract demonstrated a remarkable 95% reduction in activity. Throughout the course of this study, the chloroform extract underwent several rounds of inhibition-directed fractionation. Scheme 9 gives a detailed summary of the results from screening the acai berry extracts, highlighting fractions based on their inhibition of MCOD activity.

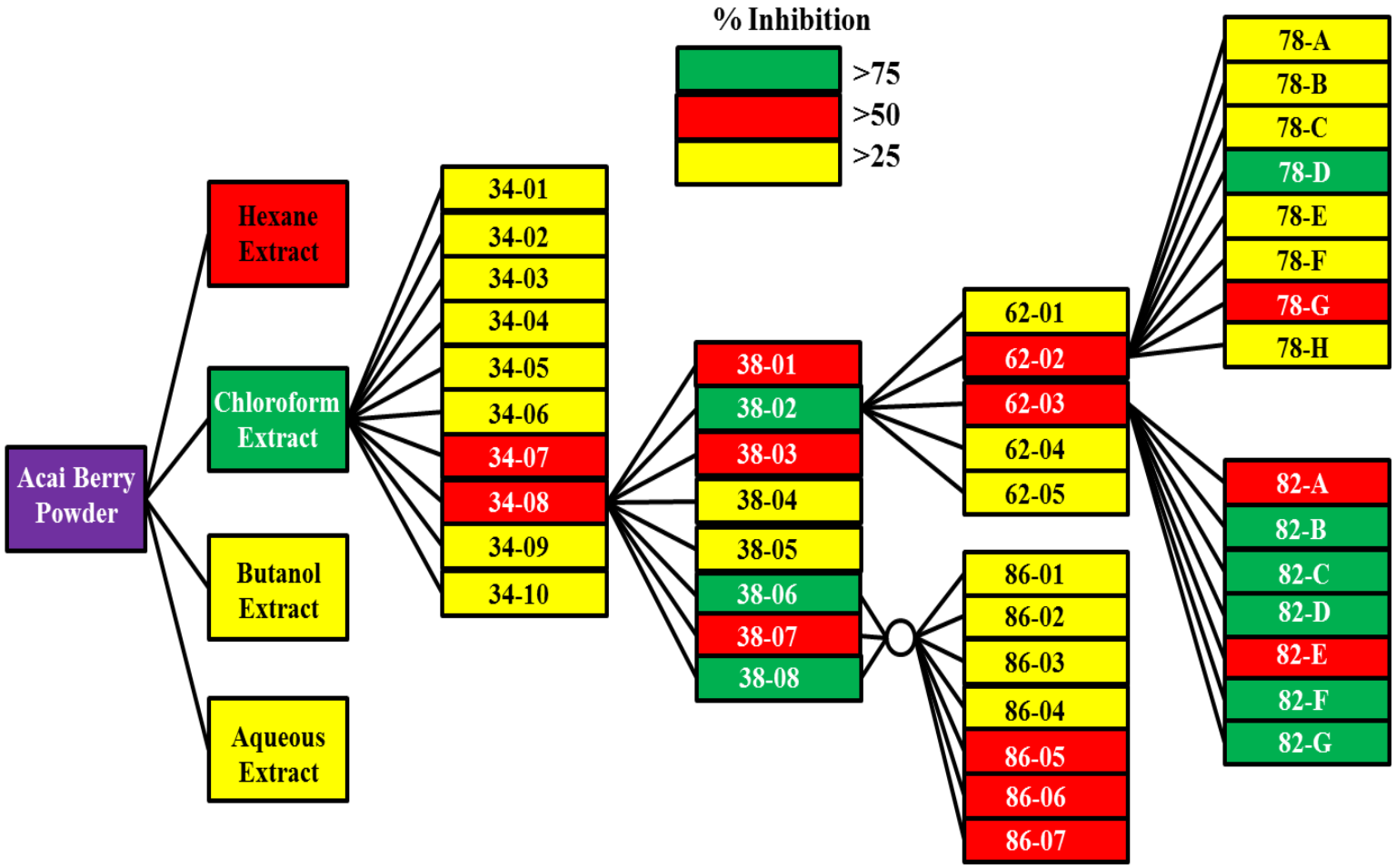

Scheme 9. Summary of Bioassay Guided Fractionation of MCOD Inhibition. Fractionation of the acai berry powder via observed reduction in 7-methoxycoumarin O-demethylation activity in the presence of human hepatic S9 fractions.

As discussed in the Results and Discussion section, several later-stage fractions underwent further experimentation. During this phase of the study, the major constituent in the 78-D fraction was determined to be 1-9-hexadecenoate (Figure 32), a monounsaturated fatty acid. A large number of CYP450 isoforms participate in the endogenous metabolism of lipids in the body. For example, CYP2E1 is responsible for the activation of arachidonic acid, the polyunsaturated fatty acid precursor to a variety of CNS signaling molecules, and epoxyeicosatrienoic acid, a vasodilation and anti-inflammatory signaling precursor[72]. However, it should be noted that the role fatty acids play in cytochrome P450 inhibition has not been thoroughly studied. Yao et al recently investigated a wide range of fatty acids for CYP450 inhibition. Results from this study showed that the polyunsaturated fatty acids arachidonic acid, eicosapentaenoic acid, and docosahexaenoic acid were potent inhibitors of CYP2C9 and 2C19 (K_i<5 µM) and weak inhibitors of CYP3A4, 1A2, and 2E1 (K_i >10 µM)[73]. Given the relatively high K_i of 1-9-hexadecenoate (73 µM), it can be classified as a weak inhibitor of human cytochrome P450. Future studies might reveal constituents in the acai berry with more potent inhibition.

The 7-methoxycoumarin O-demethylation assay proved to be useful tool for the non-selective screening several human cytochrome P450 isoforms. With the implication that the acai berry inhibits these CYP450 isoforms, there exists a potential for innumerable herbal-drug interactions. Studies have shown that the CYP1A2 metabolism of warfarin, an anticoagulant, is susceptible to large number of botanical interactions, including soy milk[74], ginseng[75], and foods rich in vitamin k_1[76]. Hemorrhaging results

from an increase in international normalization ratio (INR), which is a measure of the tendency for blood to clot and is directly affected by warfarin bioavailability[77]. Inhibition of CYP2E1 metabolism can actually prevent adverse effects on the body. Most notably, CYP2E1 oxidation of acetaminophen can result in the formation of N-acetyl-p-benzoquininemine, a hepatotoxic metabolite. Inhibition of 2E1 would be beneficial when a high dosage of acetaminophen is present in the body[78].

In summary, weak interactions have been observed using the general CYP450 probe substrate 7-methoxycoumarin, and several fractions have been identified as potential inhibitors, one being identified as a fatty acid with a K_i of approximately 73 μM. The current study also demonstrates that acai berry fractions do not appear to interact substantially with the two major drug metabolizing families 3A and 2D, which metabolize a large percentage of all pharmaceuticals on the market, and this suggests a low potential for adverse drug interactions related to consumption of acai berry products. Additional studies are currently on-going to address P450 isoforms that were not represented in this study.

REFERENCES

1. Ding, X.; Kaminsky, L. S., Human extrahepatic cytochromes P450: function in xenobiotic metabolism and tissue-selective chemical toxicity in the respiratory and gastrointestinal tracts. *Annu Rev Pharmacol Toxicol* **2003,** *43*, 149-73.
2. Pirmohamed, M.; Kitteringham, N. R.; Park, B. K., The role of active metabolites in drug toxicity. *Drug Saf* **1994,** *11* (2), 114-44.
3. Anzenbacher, P.; Anzenbacherová, E., Cytochrome P450 and metabolism of xenobiotics. *Cell. Mol. Life Sci.* **2001,** *58* (5), 737-747.
4. Krishna, D. R.; Klotz, U., Extrahepatic metabolism of drugs in humans. *Clin Pharmacokinet* **1994,** *26* (2), 144-60.
5. Denisov, I. G.; Makris, T. M.; Sligar, S. G.; Schlichting, I., Structure and chemistry of cytochrome P450. *Chem Rev* **2005,** *105* (6), 2253-77.
6. Nelson, D. R.; Koymans, L.; Kamataki, T.; Stegeman, J. J.; Feyereisen, R.; Waxman, D. J.; Waterman, M. R.; Gotoh, O.; Coon, M. J.; Estabrook, R. W.; Gunsalus, I. C.; Nebert, D. W., P450 superfamily: update on new sequences, gene mapping, accession numbers and nomenclature. *Pharmacogenetics* **1996,** *6* (1), 1-42.
7. Tuck, S. F.; Graham-Lorence, S.; Peterson, J. A.; Ortiz de Montellano, P. R., Active sites of the cytochrome p450cam (CYP101) F87W and F87A mutants. Evidence for significant structural reorganization without alteration of catalytic regiospecificity. *J Biol Chem* **1993,** *268* (1), 269-75.
8. Ohkura, K.; Kawaguchi, Y.; Watanabe, Y.; Masubuchi, Y.; Shinohara, Y.; Hori, H., Flexible structure of cytochrome P450: promiscuity of ligand binding in the CYP3A4 heme pocket. *Anticancer Res* **2009,** *29* (3), 935-42.
9. Raunio, H.; Rautio, A.; Gullstén, H.; Pelkonen, O., Polymorphisms of CYP2A6 and its practical consequences. *Br J Clin Pharmacol* **2001,** *52* (4), 357-63.
10. Sheweita, S. A., Drug-metabolizing enzymes: mechanisms and functions. *Curr Drug Metab* **2000,** *1* (2), 107-32.
11. Meunier, B.; de Visser, S. P.; Shaik, S., Mechanism of oxidation reactions catalyzed by cytochrome p450 enzymes. *Chem Rev* **2004,** *104* (9), 3947-80.
12. Guengerich, F. P., Cytochrome p450 and chemical toxicology. *Chem Res Toxicol* **2008,** *21* (1), 70-83.
13. Meunier, B.; Adam, W., *Metal-oxo and metal-peroxo species in catalytic oxidations*. Springer: Berlin ; New York, 2000; p viii, 323 p.
14. Groves, J. T., Models and Mechanisms of Cytochrome P450 Action. In *Cytochrome P450*, 3rd ed.; de Montellano, P. O., Ed. Spriger US: New York, 2005; pp 1-43.
15. De Montellano, O.; De Voss, J., Oxidizing species in the mechanism of cytochrome P450. *Nat. Prod. Rep.* **2002,** *19* (4), 477-493

16. Huang, S. M.; Strong, J. M.; Zhang, L.; Reynolds, K. S.; Nallani, S.; Temple, R.; Abraham, S.; Habet, S. A.; Baweja, R. K.; Burckart, G. J.; Chung, S.; Colangelo, P.; Frucht, D.; Green, M. D.; Hepp, P.; Karnaukhova, E.; Ko, H. S.; Lee, J. I.; Marroum, P. J.; Norden, J. M.; Qiu, W.; Rahman, A.; Sobel, S.; Stifano, T.; Thummel, K.; Wei, X. X.; Yasuda, S.; Zheng, J. H.; Zhao, H.; Lesko, L. J., New era in drug interaction evaluation: US Food and Drug Administration update on CYP enzymes, transporters, and the guidance process. *J Clin Pharmacol* **2008,** *48* (6), 662-70.
17. Paine, M. F.; Hart, H. L.; Ludington, S. S.; Haining, R. L.; Rettie, A. E.; Zeldin, D. C., The human intestinal cytochrome P450 "pie". *Drug Metab Dispos* **2006,** *34* (5), 880-6.
18. Wrighton, S. A.; Maurel, P.; Schuetz, E. G.; Watkins, P. B.; Young, B.; Guzelian, P. S., Identification of the cytochrome P-450 induced by macrolide antibiotics in rat liver as the glucocorticoid responsive cytochrome P-450p. *Biochemistry* **1985,** *24* (9), 2171-8.
19. Cholerton, S.; Daly, A. K.; Idle, J. R., The role of individual human cytochromes P450 in drug metabolism and clinical response. *Trends Pharmacol Sci* **1992,** *13* (12), 434-9.
20. Correia, M.; De Montellano, P., Inhibition of Cytochrome P450 Enzymes. In *Cytochrome P450*, 3rd ed.; de Montellano, P., Ed. Springer US: New York, 2005; pp 247-280.
21. Guengerich, F., Human Cytochrome P450 Enzymes: P450 3A4. In *Cytochrome P450*, 3rd ed.; Springer US: New York, 2005; pp 473-535.
22. Ballantyne, C. M.; Corsini, A.; Davidson, M. H.; Holdaas, H.; Jacobson, T. A.; Leitersdorf, E.; März, W.; Reckless, J. P.; Stein, E. A., Risk for myopathy with statin therapy in high-risk patients. *Arch Intern Med* **2003,** *163* (5), 553-64.
23. Flockhart, D. Drug Interactions: Cytochrome P450 Drug Interaction Table. *http://medicine.iupui.edu/clinpharm/ddis/clinical-table/*.
24. Guengerich, F., Human Cytochrome P450 Enzymes. In *Cytochrome P450*, 3rd ed.; De Montellano, P., Ed. Springer US: New York, 2005; pp 473-535
25. Lynch, T.; Price, A., The effect of cytochrome P450 metabolism on drug response, interactions, and adverse effects. *Am Fam Physician* **2007,** *76* (3), 391-6.
26. Parker, R. B.; Soberman, J. E., Effects of paroxetine on the pharmacokinetics and pharmacodynamics of immediate-release and extended-release metoprolol. *Pharmacotherapy* **2011,** *31* (7), 630-41.
27. Duricova, J.; Perinova, I.; Jurckova, N.; Jeziskova, I.; Kacirova, I.; Grundmann, M., Cytochrome P450 2D6 phenotype and genotype in hypertensive patients on long-term therapy with metoprolol. *Bratisl Lek Listy* **2013,** *114* (4), 206-12.
28. Ward, B. A.; Gorski, J. C.; Jones, D. R.; Hall, S. D.; Flockhart, D. A.; Desta, Z., The cytochrome P450 2B6 (CYP2B6) is the main catalyst of efavirenz primary and secondary metabolism: implication for HIV/AIDS therapy and utility of efavirenz as a substrate marker of CYP2B6 catalytic activity. *J Pharmacol Exp Ther* **2003,** *306* (1), 287-300.
29. Woodhouse, K. W.; Mitchison, H. C.; Mutch, E.; Wright, P. D.; Rawlins, M. D.; James, O. F., The metabolism of 7-ethoxycoumarin in human liver microsomes and the

effect of primary biliary cirrhosis: implications for studies of drug metabolism in liver disease. *Br J Clin Pharmacol* **1985,** *20* (1), 77-80.
30. Pelkonen, O.; Pasanen, M.; Kuha, H.; Gachalyi, B.; Kairaluoma, M.; Sotaniemi, E. A.; Park, S. S.; Friedman, F. K.; Gelboin, H. V., The effect of cigarette smoking on 7-ethoxyresorufin O-deethylase and other monooxygenase activities in human liver: analyses with monoclonal antibodies. *Br J Clin Pharmacol* **1986,** *22* (2), 125-34.
31. Brahmachari, G., *Mother nature — an inexhaustible source of drugs and lead molecules* Narosa Publishing House: New Delhi, India, 2009.
32. Kakar, S. M.; Paine, M. F.; Stewart, P. W.; Watkins, P. B., 6'7'-Dihydroxybergamottin contributes to the grapefruit juice effect. *Clin Pharmacol Ther* **2004,** *75* (6), 569-79.
33. Paine, M. F.; Criss, A. B.; Watkins, P. B., Two major grapefruit juice components differ in time to onset of intestinal CYP3A4 inhibition. *J Pharmacol Exp Ther* **2005,** *312* (3), 1151-60.
34. Paine, M. F.; Widmer, W. W.; Hart, H. L.; Pusek, S. N.; Beavers, K. L.; Criss, A. B.; Brown, S. S.; Thomas, B. F.; Watkins, P. B., A furanocoumarin-free grapefruit juice establishes furanocoumarins as the mediators of the grapefruit juice-felodipine interaction. *Am J Clin Nutr* **2006,** *83* (5), 1097-105.
35. Udani, J. K.; Singh, B. B.; Singh, V. J.; Barrett, M. L., Effects of Açai (Euterpe oleracea Mart.) berry preparation on metabolic parameters in a healthy overweight population: a pilot study. *Nutr J* **2011,** *10*, 45.
36. Mertens-Talcott, S. U.; Rios, J.; Jilma-Stohlawetz, P.; Pacheco-Palencia, L. A.; Meibohm, B.; Talcott, S. T.; Derendorf, H., Pharmacokinetics of anthocyanins and antioxidant effects after the consumption of anthocyanin-rich acai juice and pulp (Euterpe oleracea Mart.) in human healthy volunteers. *J Agric Food Chem* **2008,** *56* (17), 7796-802.
37. Dreiseitel, A.; Schreier, P.; Oehme, A.; Locher, S.; Hajak, G.; Sand, P. G., Anthocyanins and their metabolites are weak inhibitors of cytochrome P450 3A4. *Mol Nutr Food Res* **2008,** *52* (12), 1428-33.
38. Phillipson, D. W.; Milgram, K. E.; Yanovsky, A. I.; Rusnak, L. S.; Haggerty, D. A.; Farrell, W. P.; Greig, M. J.; Xiong, X.; Proefke, M. L., High-throughput bioassay-guided fractionation: a technique for rapidly assigning observed activity to individual components of combinatorial libraries, screened in HTS bioassays. *J Comb Chem* **2002,** *4* (6), 591-9.
39. Weller, M. G., A unifying review of bioassay-guided fractionation, effect-directed analysis and related techniques. *Sensors (Basel)* **2012,** *12* (7), 9181-209.
40. Junio, H. A.; Sy-Cordero, A. A.; Ettefagh, K. A.; Burns, J. T.; Micko, K. T.; Graf, T. N.; Richter, S. J.; Cannon, R. E.; Oberlies, N. H.; Cech, N. B., Synergy-directed fractionation of botanical medicines: a case study with goldenseal (Hydrastis canadensis). *J Nat Prod* **2011,** *74* (7), 1621-9.
41. Miller, K.; Neilan, B.; Sze, D. M., Development of Taxol and other endophyte produced anti-cancer agents. *Recent Pat Anticancer Drug Discov* **2008,** *3* (1), 14-9.

42. Oberlies, N. H.; Kroll, D. J., Camptothecin and taxol: historic achievements in natural products research. *J Nat Prod* **2004,** *67* (2), 129-35.
43. Oberlies, N. H.; Rogers, L. L.; Martin, J. M.; McLaughlin, J. L., Cytotoxic and insecticidal constituents of the unripe fruit of Persea americana. *J Nat Prod* **1998,** *61* (6), 781-5.
44. Khan, A. J.; Sharma, A.; Choudhuri, G.; Parmar, D., Induction of blood lymphocyte cytochrome P450 2E1 in early stage alcoholic liver cirrhosis. *Alcohol* **2011,** *45* (1), 81-7.
45. Clarke, T. A.; Waskell, L. A., The metabolism of clopidogrel is catalyzed by human cytochrome P450 3A and is inhibited by atorvastatin. *Drug Metab Dispos* **2003,** *31* (1), 53-9.
46. Su, T.; Bao, Z.; Zhang, Q. Y.; Smith, T. J.; Hong, J. Y.; Ding, X., Human cytochrome P450 CYP2A13: predominant expression in the respiratory tract and its high efficiency metabolic activation of a tobacco-specific carcinogen, 4-(methylnitrosamino)-1-(3-pyridyl)-1-butanone. *Cancer Res* **2000,** *60* (18), 5074-9.
47. Compton, B.; Purdy, W., The mechanism of the reaction of the Nash and the Sawicki aldehyde reagent. *Can. J. Chem.* **1980,** *58*, 2207-2211.
48. Minamiyama, Y.; Takemura, S.; Akiyama, T.; Imaoka, S.; Inoue, M.; Funae, Y.; Okada, S., Isoforms of cytochrome P450 on organic nitrate-derived nitric oxide release in human heart vessels. *FEBS Lett* **1999,** *452* (3), 165-9.
49. Koley, A. P.; Dai, R.; Robinson, R. C.; Markowitz, A.; Friedman, F. K., Differential interaction of erythromycin with cytochromes P450 3A1/2 in the endoplasmic reticulum: a CO flash photolysis study. *Biochemistry* **1997,** *36* (11), 3237-41.
50. Minocha, M.; Mandava, N. K.; Kwatra, D.; Pal, D.; Folk, W. R.; Earla, R.; Mitra, A. K., Effect of short term and chronic administration of Sutherlandia frutescens on pharmacokinetics of nevirapine in rats. *Int J Pharm* **2011,** *413* (1-2), 44-50.
51. Imaoka, S.; Terano, Y.; Funae, Y., Constitutive testosterone 6 beta-hydroxylase in rat liver. *J Biochem* **1988,** *104* (3), 481-7.
52. Kato, R.; Yamashita, S.; Moriguchi, J.; Nakagawa, M.; Tsukura, Y.; Uchida, K.; Amano, F.; Hirotani, Y.; Ijiri, Y.; Tanaka, K., Changes of midazolam pharmacokinetics in Wistar rats treated with lipopolysaccharide: relationship between total CYP and CYP3A2. *Innate Immun* **2008,** *14* (5), 291-7.
53. Tomkins, D. M.; Otton, S. V.; Joharchi, N.; Li, N. Y.; Balster, R. F.; Tyndale, R. F.; Sellers, E. M., Effect of cytochrome P450 2D1 inhibition on hydrocodone metabolism and its behavioral consequences in rats. *J Pharmacol Exp Ther* **1997,** *280* (3), 1374-82.
54. Miksys, S.; Rao, Y.; Sellers, E. M.; Kwan, M.; Mendis, D.; Tyndale, R. F., Regional and cellular distribution of CYP2D subfamily members in rat brain. *Xenobiotica* **2000,** *30* (6), 547-64.
55. Tyndale, R. F.; Li, Y.; Li, N. Y.; Messina, E.; Miksys, S.; Sellers, E. M., Characterization of cytochrome P-450 2D1 activity in rat brain: high-affinity kinetics for dextromethorphan. *Drug Metab Dispos* **1999,** *27* (8), 924-30.

56. Schmider, J.; Greenblatt, D. J.; Fogelman, S. M.; von Moltke, L. L.; Shader, R. I., Metabolism of dextromethorphan in vitro: involvement of cytochromes P450 2D6 and 3A3/4, with a possible role of 2E1. *Biopharm Drug Dispos* **1997,** *18* (3), 227-40.
57. Lake, B. G., Coumarin metabolism, toxicity and carcinogenicity: relevance for human risk assessment. *Food Chem Toxicol* **1999,** *37* (4), 423-53.
58. O'Reilly, R. A., Studies on the coumarin anticoagulant drugs: interaction of human plasma albumin and warfarin sodium. *J Clin Invest* **1967,** *46* (5), 829-37.
59. Reen, R. K.; Ramakanth, S.; Wiebel, F. J.; Jain, M. P.; Singh, J., Dealkylation of 7-methoxycoumarin as assay for measuring constitutive and phenobarbital-inducible cytochrome P450s. *Anal Biochem* **1991,** *194* (2), 243-9.
60. Matsubara, T.; Yoshihara, E.; Iwata, T.; Tochino, Y.; Hachino, Y., Biotransformation of coumarin derivatives (1). 7-alkoxycoumarin O-dealkylase in liver microsomes. *Jpn J Pharmacol* **1982,** *32* (1), 9-21.
61. Czekaj, P., Phenobarbital-induced expression of cytochrome P450 genes. *Acta Biochim Pol* **2000,** *47* (4), 1093-105.
62. Forrester, L. M.; Henderson, C. J.; Glancey, M. J.; Back, D. J.; Park, B. K.; Ball, S. E.; Kitteringham, N. R.; McLaren, A. W.; Miles, J. S.; Skett, P., Relative expression of cytochrome P450 isoenzymes in human liver and association with the metabolism of drugs and xenobiotics. *Biochem J* **1992,** *281 (Pt 2)*, 359-68.
63. Kim, D.; Wu, Z. L.; Guengerich, F. P., Analysis of coumarin 7-hydroxylation activity of cytochrome P450 2A6 using random mutagenesis. *J Biol Chem* **2005,** *280* (48), 40319-27.
64. Cholerton, S.; Idle, M. E.; Vas, A.; Gonzalez, F. J.; Idle, J. R., Comparison of a novel thin-layer chromatographic-fluorescence detection method with a spectrofluorometric method for the determination of 7-hydroxycoumarin in human urine. *J Chromatogr* **1992,** *575* (2), 325-30.
65. Dreiseitel, A.; Schreier, P.; Oehme, A.; Locher, S.; Rogler, G.; Piberger, H.; Hajak, G.; Sand, P. G., Anthocyanins and anthocyanidins are poor inhibitors of CYP2D6. *Methods Find Exp Clin Pharmacol* **2009,** *31* (1), 3-9.
66. Dierks, E. A.; Stams, K. R.; Lim, H. K.; Cornelius, G.; Zhang, H.; Ball, S. E., A method for the simultaneous evaluation of the activities of seven major human drug-metabolizing cytochrome P450s using an in vitro cocktail of probe substrates and fast gradient liquid chromatography tandem mass spectrometry. *Drug Metab Dispos* **2001,** *29* (1), 23-9.
67. He, K.; Iyer, K. R.; Hayes, R. N.; Sinz, M. W.; Woolf, T. F.; Hollenberg, P. F., Inactivation of cytochrome P450 3A4 by bergamottin, a component of grapefruit juice. *Chem Res Toxicol* **1998,** *11* (4), 252-9.
68. Oetari, S.; Sudibyo, M.; Commandeur, J. N.; Samhoedi, R.; Vermeulen, N. P., Effects of curcumin on cytochrome P450 and glutathione S-transferase activities in rat liver. *Biochem Pharmacol* **1996,** *51* (1), 39-45.
69. Mohutsky, M. A.; Anderson, G. D.; Miller, J. W.; Elmer, G. W., Ginkgo biloba: evaluation of CYP2C9 drug interactions in vitro and in vivo. *Am J Ther* **2006,** *13* (1), 24-31.

70. Jiang, X.; Williams, K. M.; Liauw, W. S.; Ammit, A. J.; Roufogalis, B. D.; Duke, C. C.; Day, R. O.; McLachlan, A. J., Effect of ginkgo and ginger on the pharmacokinetics and pharmacodynamics of warfarin in healthy subjects. *Br J Clin Pharmacol* **2005,** *59* (4), 425-32.
71. Uchida, S.; Yamada, H.; Li, X. D.; Maruyama, S.; Ohmori, Y.; Oki, T.; Watanabe, H.; Umegaki, K.; Ohashi, K.; Yamada, S., Effects of Ginkgo biloba extract on pharmacokinetics and pharmacodynamics of tolbutamide and midazolam in healthy volunteers. *J Clin Pharmacol* **2006,** *46* (11), 1290-8.
72. Porubsky, P. R.; Battaile, K. P.; Scott, E. E., Human cytochrome P450 2E1 structures with fatty acid analogs reveal a previously unobserved binding mode. *J Biol Chem* **2010,** *285* (29), 22282-90.
73. Yao, H. T.; Chang, Y. W.; Lan, S. J.; Chen, C. T.; Hsu, J. T.; Yeh, T. K., The inhibitory effect of polyunsaturated fatty acids on human CYP enzymes. *Life Sci* **2006,** *79* (26), 2432-40.
74. Cambria-Kiely, J. A., Effect of soy milk on warfarin efficacy. *Ann Pharmacother* **2002,** *36* (12), 1893-6.
75. Rosado, M. F., Thrombosis of a prosthetic aortic valve disclosing a hazardous interaction between warfarin and a commercial ginseng product. *Cardiology* **2003,** *99* (2), 111.
76. Qureshi, G. D.; Reinders, T. P.; Swint, J. J.; Slate, M. B., Acquired warfarin resistance and weight-reducing diet. *Arch Intern Med* **1981,** *141* (4), 507-9.
77. Hirsh, J.; Dalen, J.; Anderson, D. R.; Poller, L.; Bussey, H.; Ansell, J.; Deykin, D., Oral anticoagulants: mechanism of action, clinical effectiveness, and optimal therapeutic range. *Chest* **2001,** *119* (1 Suppl), 8S-21S.
78. Lee, S. S.; Buters, J. T.; Pineau, T.; Fernandez-Salguero, P.; Gonzalez, F. J., Role of CYP2E1 in the hepatotoxicity of acetaminophen. *J Biol Chem* **1996,** *271* (20), 12063-7.